TURBOMACHINERY & PUMP SYMPOSIA | HOUSTON, TX
SEPTEMBER 15-17, 2020
SHORT COURSES: SEPTEMBER 14, 2020

WHY MACHINES FAIL TO FOLLOW TEXTBOOK STATED RULES, AS ILLUSTRATED BY SHAFT CRACK AND ROTOR SELF EXCITED VIBRATION CASES IN CRITICAL MACHINERY

Piotr Miałkowski, PhD
Machinery Diagnostic Services Technical Leader, Central and Eastern Europe
Baker Hughes - Bently Nevada
Poland

Nicolas Péton, PhD
Machinery Diagnostic Services Global Director
Baker Hughes - Bently Nevada
France

Peter Popaleny, PhD
Machinery Diagnostic Services Technical Leader, West Europe
Baker Hughes - Bently Nevada
Slovakia

This tutorial demonstrates some aspects of rotating machinery diagnostics where there is an apparent difference between the actual response of a machine and its expected behavior for a certain type of malfunction as typically found in industry analyst training courses. This tutorial concentrates on two of the most devasting malfunctions: shaft cracks and fluid film instabilities. The seriousness of these two malfunctions demands the immediate attention by the analyst to quickly determine before the potential catastrophic and terminal results. The reason of selecting these two is because both are serious and potentially terminal problems. From another perspective these malfunctions are on opposite ends of the vibration based diagnostics path. The shaft crack grows slowly and is a forced vibration problem related to the condition of a single machine part (rotor), whereas fluid film induced instabilities are invariably an instantaneous phenomenon that causes self-excited vibrations of high enough to trip the machine. However, a common factor for both malfunctions is that a maintenance experts say these malfunctions are relatively rare phenomena. As a result, to identify faults correctly, diagnostic engineers must rely on analyst training courses and published case history literature, rather than on personal experience. For both malfunctions we start with a short presentation of the diagnostics methodology, as used in the service organization the authors are employed, followed by a discussion of the practical implementation of this methodology along with selected machinery case studies.

PART I. SHAFT CRACK

Shaft crack is a slowly growing fracture of the rotor. If undetected, it will grow until the remaining cross section of the rotor cannot withstand acting loads and the rotor fails in a brittle fracture mode. A rotating system holds a lot of stored energy, and when this energy releases within a short time, the result is usually catastrophic because of secondary damage due to liberated parts or rotor section components. Since we will be talking about machines equipped with proper monitoring and protection systems, this final stage is not in our area of interest. The crack should be detected at an earlier stage, during the fatigue period when the crack propagating (growing). The diagnostic methodology outlined here is based on Ref. [1], unless stated otherwise, and it requires the long term monitoring of the machine, looking for changes in the 1X (component filtered to rotating speed frequency) and 2X (component filtered to twice rotating speed frequency) vibration vectors. Other machine malfunctions (unbalance, misalignment, loose rotating part, rub) also cause changes to the 1X and/or 2X vibration vectors. These other machine malfunctions must be reviewed and rejected to pursue the two rules for shaft crack. When teaching diagnostic engineers two basic rules are usually presented as related to the 1X and 2X activity in a cracked rotor response:

Rule #1: If rotor is cracked, it is almost certainly bowed.

Rule #2: If a crack causes asymmetry in the rotor lateral stiffness, and if the rotor supports a radial static load, then strong 2X vibration will occur as 2X traverses a shaft critical speed (i.e when shaft speed equal to ½ of any resonance speed).

Rule #1 is based on the fact, that when a cross section area of the shaft is reduced, the shaft bending stiffness lowers (see Fig. 1). So, under any acting unbalance force the stiffness change will cause a change in the peak to peak displacement, i.e. 1X vibration (or dynamic bow) of the rotor. A low value of the centrifugal force may not cause a detectable change of the 1X component due to the presence of a crack (or the crack is small). Depending on a crack position, location of the original unbalance and speed of the rotor, in relation to its resonance speed, the change in the 1X vector can be in virtually any direction. Thus, when a crack propagates both amplitude and phase changes can be expected.

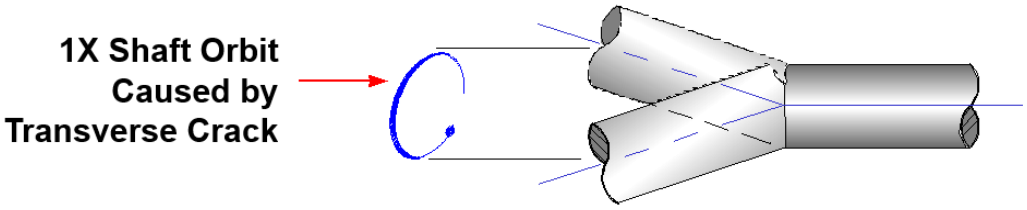

Fig.1. Rule #1 illustration – when shaft is cracked it is almost certainly bowed.

Changes to 1X vectors can be observed at low speed (slow roll), in (any) resonance region and during operating speed. Considering, that at low speed the centrifugal force from unbalance is negligible, the change of 1X slow roll vector may or may not happen. That depends on axial location of the crack versus supports location, size of already cracked surface and initial stiffness of the rotor. During steady-state operating speeds, the 1X vector acceptance region is used to monitor change in the response vector and the violations of the limit are a trigger for analysis. However, the biggest changes are expected within the resonance region: a reduced stiffness causes (with the modal mass unchanged) a reduction of the resonance frequency and increases the amplitude of vibration response in the resonance region. Moreover, if damping also reduces, there will be an increase in the (synchronous speed) amplification factor and a further raise in the resonance amplitudes when compared to a normal condition. The rotor stiffness anisotropy which may be due to a crack, subtracts from the damping. The latter provides a stabilizing effect, hence then an increase of the rotor peak amplitude response. As mentioned earlier, other machine malfunctions can change 1X response; for instance both stiffness and damping of a rotor bearing system can decrease due to an increase in bearing clearance or because of unloading in a bearing due to misalignment.

Using Rule #2 requires two conditions to be fulfilled in the same time. The first one is the presence of a static radial load acting on the rotor. In horizontal rotors one can always count on gravity load and generally for all machines there can be other radial loads like side loads from the processed medium in flow machinery, bearing reactions due to existing shaft misalignment, and so on. However, for instance in a vertical pump with radially well balanced flow, this condition may be absent.

The second prerequisite is anisotropic (i.e. asymmetric, different in radial directions) bending stiffness of the rotor (Fig.2).

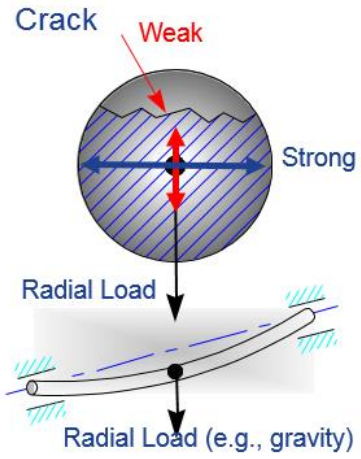

Fig.2. Illustration of prerequisites for rule#2: asymmetric radial stiffness of the rotor and an acting radial load.

Under the static radial load, the rotor bends more when the direction of the load coincides with weak stiffness axis and less when with the strong one and producing two cycles of vibration per shaft revolution, hence the 2X vibration. At half of any resonance speed this 2X component is amplified by the resonance mode, it is exciting. During diagnostic training, the instructor can demonstrate the effect

of this rule by the applying asymmetric tension of the bolts that secure the disk on the shaft of a standard one mass rotor kit. The characteristic features of vibration signal are:

Vertical relation in cascade plot (Fig.3) – the 1X and 2X components excite the resonance at the same frequency

Bode plot (Fig.4) for Direct, 1X and 2X components show the 2X resonance characteristics (maximum of amplitude and change of phase), when the rotor passed the speed at ½ of "critical speed" (i.e. resonance excited by unbalance)

Direct orbits (Fig.5) for the 2X resonance area, with characteristic internal loop changes the position, forward precession 2X component adds to normally present 1X forward orbit, due to unbalance.

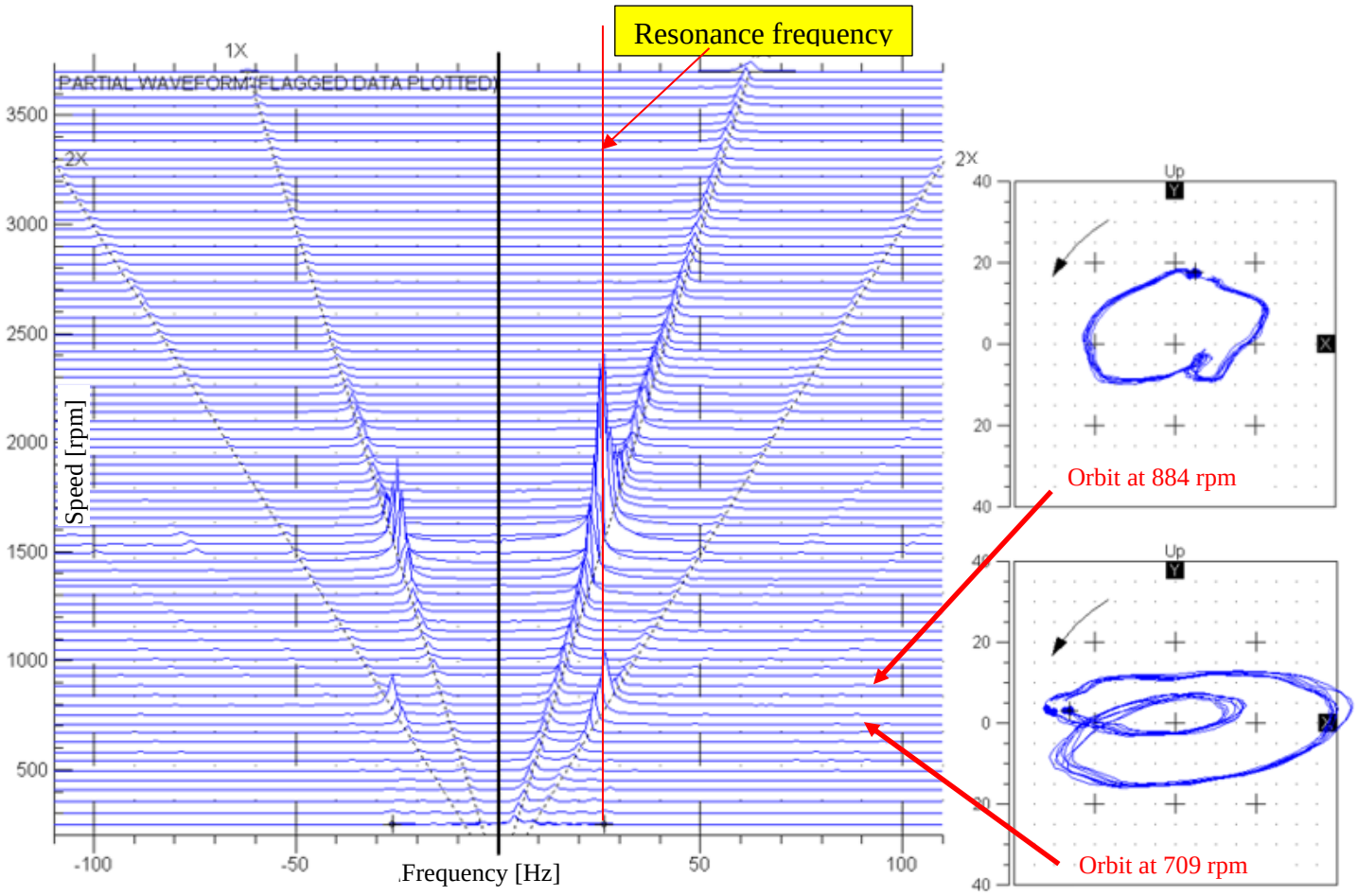

Fig. 3. Cascade plot of shaft relative vibration response for rotor kit with anisotropy of rotor stiffness. Vertical relation i.e. the same frequency of 1X and 2X excited resonances. The 2X is forward in precession.

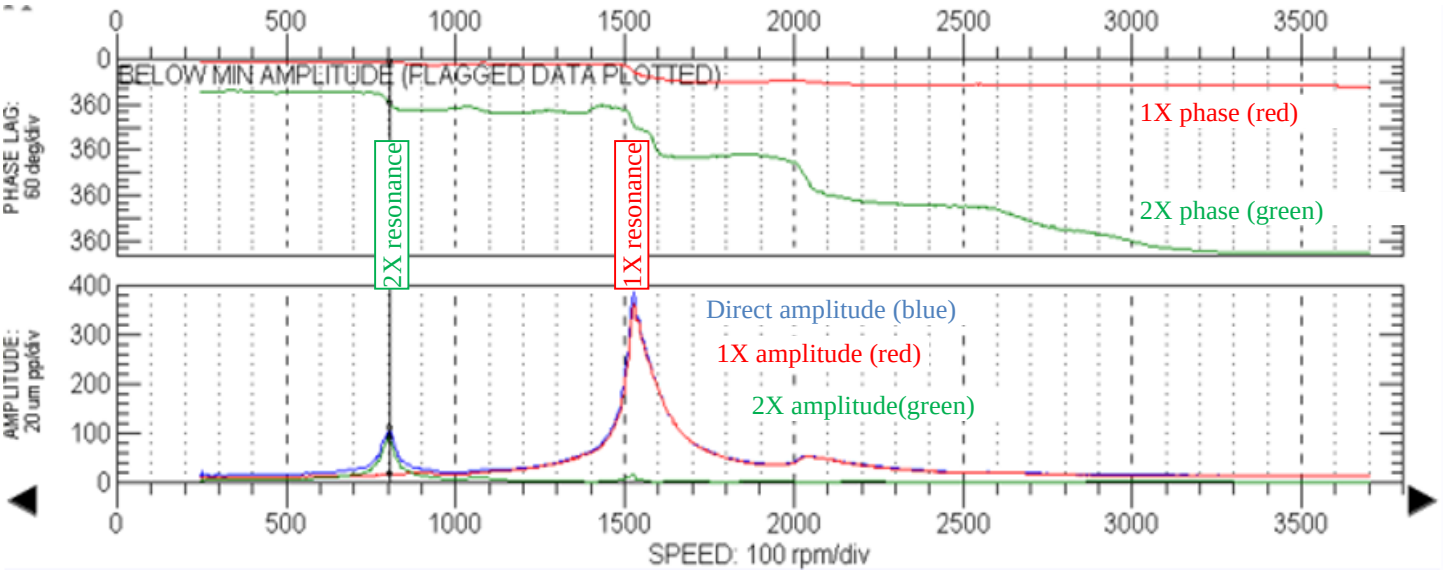

Fig.4. Bode plot for the vibration response with the 2X resonance at half of 1X resonance speed.

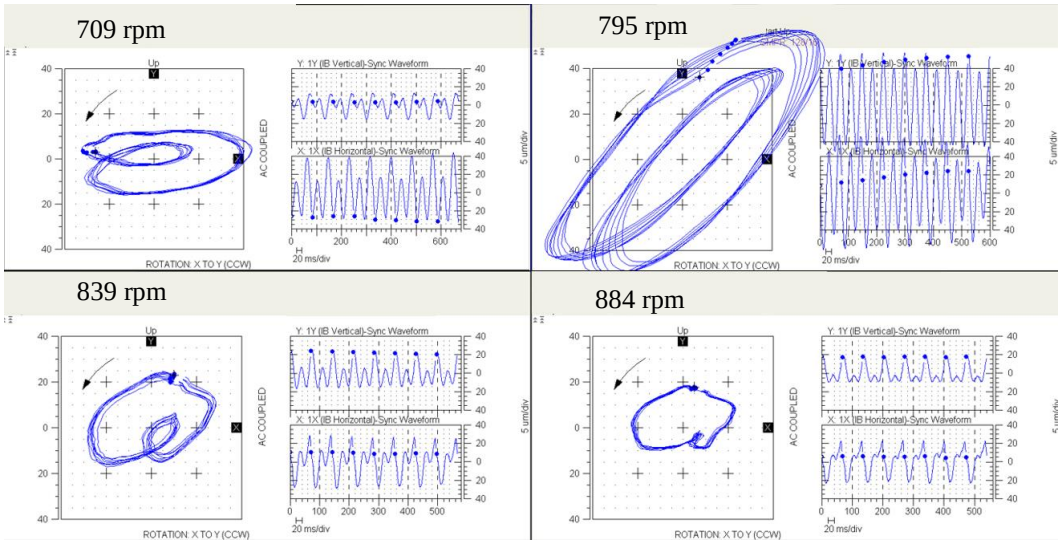

Fig.5. Sample orbits in 2X resonance region: internal loop changes position in forward direction as the rotor speed increases.

Note that the demonstration of "cracked rotor behavior" is made on a rotor that is actually not cracked. This is done on purpose. The #2 rule describes the behavior of any anisotropic rotor, no matter the cause of the anisotropy. The effect of the parametric resonance of 2X component can be seen in many 2 pole generator rotors but also in rotors with key secured hubs or disks. So, to apply it for crack detection we should talk about a change in the symptoms, i.e. trending the 2X activity. Use of acceptance regions for 2X vector is advised, note however that changes at the ½ resonance speed will be earlier and more intensive than ones at the operating speed. Note also that not every cracked rotor will exhibit the symptoms of rule #2, simply because not all cracks are introducing radial stiffness asymmetry (see Fig. 6).

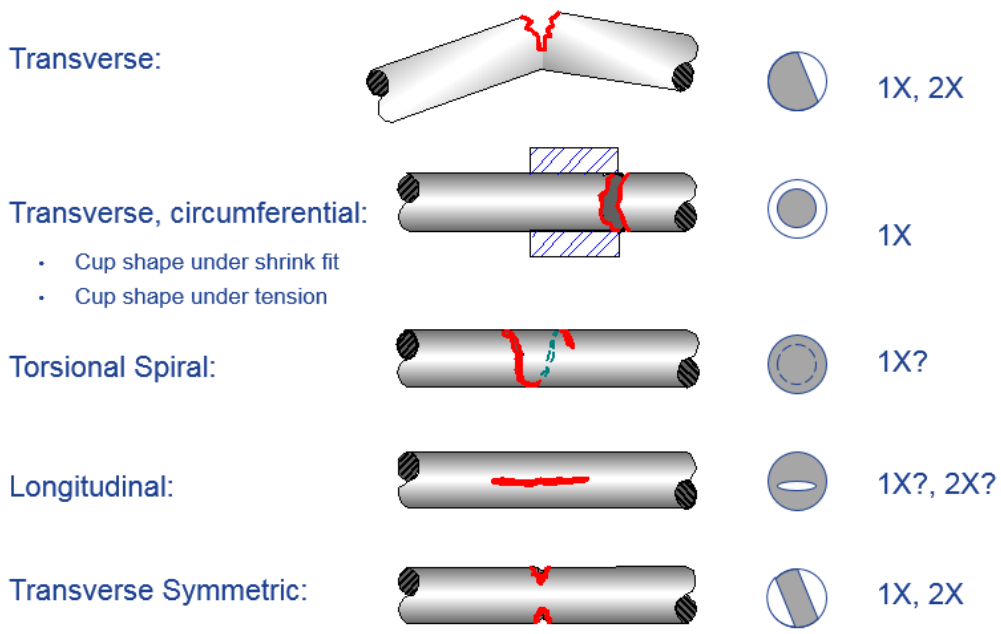

Fig.6. Sample types of crack propagation schemes and accompanying vibration effects.

For instance, torsional cracks may be difficult to detect by shaft lateral vibration monitoring (until final failure), because they do not significantly affect the shaft bending stiffness. They do however affect the torsional stiffness. Thus, if torsional vibration is measured, a decrease of the resonance frequency can be detected.

One other rule that can be stated is Rule #3, thermal sensitivity of a cracked rotor. Additionally, to the long term 1X vector changes as described in rule #1, the cracked rotors may show transient change of 1X vibration i.e. change in the dynamic bow when the temperature of the surrounding medium is changed fast enough. Consider the crack development from rotor surface, no matter if it is transverse from one side, symmetric or for example circumferential one (Fig. 7). When the temperature of the medium around the rotor is increased then, with some inertia, the rotor temperature starts to rise. But the temperature will change faster at the surface than at the core of the rotor. In consequence the thermal expansion of the metal closer to surface is higher than at the core, so for some time the crack will "close" and the stiffness of the rotor will be partially restored. When the temperature equalizes along the rotor section diameter, the crack "opens" again. Reverse process (temporary opening of the crack and reduction of the stiffness for time of thermal transient) can be expected when rotor cools down. See for instance the case of the cracked generator rotor in [2] describing the reaction of rotor vibration on the change of the coolant (hydrogen) temperature.

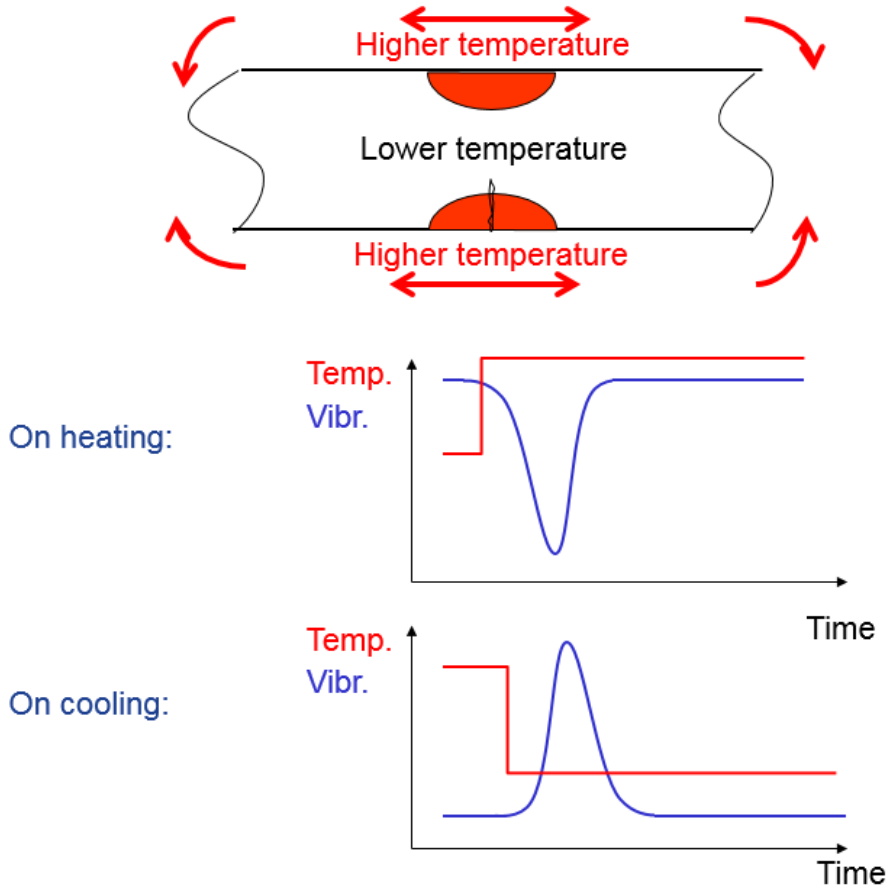

Fig.7. Cracked rotor can demonstrate transient thermal sensitivity due to fast change in surrounding media temperature.

The accumulated damage of the shaft material in the phase of fatigue crack is a function of the number of stress cycles and their amplitude. Of the two vibration effects (1X and 2X); the more destructive, assuming the same vibration amplitude, will be the effect of 2X when the stress cycles are reversal and with higher frequency. For any case the amplitudes of stress cycles increase with time on crack development. The lower is the remaining surface of the section the higher is the stress, even for the same level of acting force. The force will also rise as the vibration raises for 1X the lowered stiffness means higher dynamic deflection. The 2X component will be driven by increase of anisotropy. Due to this closed loop the development of crack accelerates. It can be temporarily slowed down by reducing forces (balancing for lower 1X and alignment for lower 2X) but the crack will continue to grow. This one-way direction of changes and exponential type characteristic of long-term vibration amplitude change are other hallmarks of shaft cracks. Actually, this is the reason that diagnosis can be done with confidence: as long as the vibrations are "just growing" then analysis and tests can be made. But when the growth becomes exponential, when the resonance characteristics significantly change from run to run, it is time to stop the machine for inspection. In the first case presented hereafter the authors highlight the story of a rotor that was operated for more than 10 months with the diagnosis of a possible rotor crack, while waiting for the new rotor to be manufactured. That was considered safe because the vibration growth was monitored in the resonance region. Analyzing pictures of the cracked areas one can see that the fatigue area was from more than 50% to almost 90% percent of the area of the section. The elevated amplitudes at operating conditions due to a growing crack result in protective shutdowns. The amplitudes will be increased during the transition through the resonance region, but the shaft is probably still in one piece. However, the protection system will continue to trip the machine on any further startups if the cracked rotor is not replaced.

Let's take a look how the diagnostic rules stated above work in-real-life situations. The cases highlight the complexity of rotor crack diagnostics as the primary problem as it can be often masked by other existing machine malfunctions, such as unbalance, misalignment, bearing looseness or soft foot.

FIRST CASE:

Introduction

The combined cycle train consists of a 177 MW, 3000 rpm generator driven by a gas turbine and steam turbine utilizing exhaust heat from the gas turbine unit (Fig 8). The steam turbine was claimed to have a dynamic problem because of changes in vibration behavior (1X vibration changes). This case is based on Dr. Peter Popaleny, author of this paper, dissertation thesis [9].

The steam turbine is a condensing type with downward flow exhaust. The inlet emergency stop valve is separated from control valves. Two control valves are integrated on the turbine cylinder casing. The steam turbine rotor (Fig. 8) is machined from a solid forging of alloy steel. The rotor is machined to form a balance piston, which is designed to balance the thrust on the blading and to reduce the thrust load supported by the thrust bearing at any operating condition. The reduced clearances necessary to control the steam leakages are maintained by seal strips. The rotor is supported by two tilting pad bearings (5-pads, Load Between Pivots) located in the bearing housing. The front-end pedestal (DE bearing 1) of HP casing contains the thrust bearing. This is designed as a double-sided tilting pads and leveling plate's type bearing, which automatically distributes the load equally among the pads. The drive end (DE) bearing 1 is mounted on the concrete foundation which results in a high support stiffness. The non-drive end (NDE) bearing 2 is mounted on the turbine casing, inside the turbine diffuser which results in a lower support stiffness than bearing 1. Each bearing is equipped with two proximity transducers (Brg1: XE-201, YE-201; Brg2: XE-200; YE-200) in X-Y configuration, mounted 90° degrees apart, to measure shaft relative vibration. Additionally, two velocity transducers (Brg1: VE-201A, VE-201B; Brg2: VE-200A; VE-200B) are mounted on the bearing casings in the same orientation as the proximity transducers.

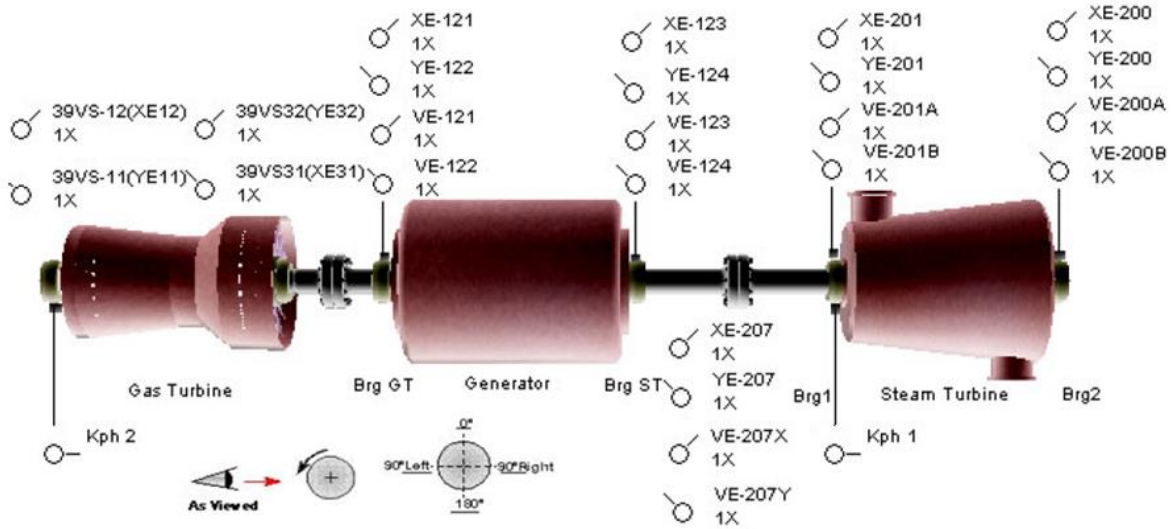

Fig.8. Machine Train Diagram showing the location of vibration transducers.

What is the historical background of the case?

- June 2008, regular overhaul after 10 years and 118 starts
- January 2009, after 89 starts in half a year, vibration increase after 3 hours of operation
- Vibration levels reach 300 um pp (12 mil pp)
- Pedestal casing expansion difference ~1.0 mm (39 mil)(L/R)
- April 2009, steam turbine overhauled again
- Rubbing found on the mid plane section seals
- Wear found under brg 2 pedestal
- Eccentricity measured in 16 radial planes, circumferentially every 45 deg
- Increased eccentricity. (0.1 mm) near brg 1 on 180–225 deg from kph notch
- Non-Destructive Test (NDT) and ultrasonic test performed on the rotor - no cracks detected

Operators had noted that the mode of operation changed for this machine, which originally operated continuously as a baseload unit. Recently, however, the unit was used as a peak load unit; and in half a year had almost as many startup/shutdown cycles as during the previous 10 years. The turbine had actually already reached the number of transients as a rotor does in 20 years of operation. When evaluating the rotor remaining life, not only the hours in operation but also the number of thermal transients (thermal stress cycles) need

to be taken into account.

This machine had high 1X vibration, but there could have been problems other than crack, for instance, the high difference in thermal expansion suggests there is a casing deformation and that can lead to rub condition and thermal bowing. The turbine was overhauled and many problems corrected. The rotor was checked for its static bending line (eccentricity measurement) by measuring the shaft line after rotation every 45º in 16 different radial planes along the rotor.

Comparison of plots during transient states

How does Rule #1 apply?

Fig. 9 contains the uncompensated 1X Bode plots of shaft relative vibration for the steam turbine bearings. The Bode plots show a difference in the slow-roll vectors, mainly on DE bearing 1 (YE-201). The slow roll vectors from a startup in 2009 are significantly (3 times) higher than from a startup in 2008. Increased 1X slow roll vectors indicate increased rotor bow due to a crack propagation, with the assumption that the rotor runout had not changed.

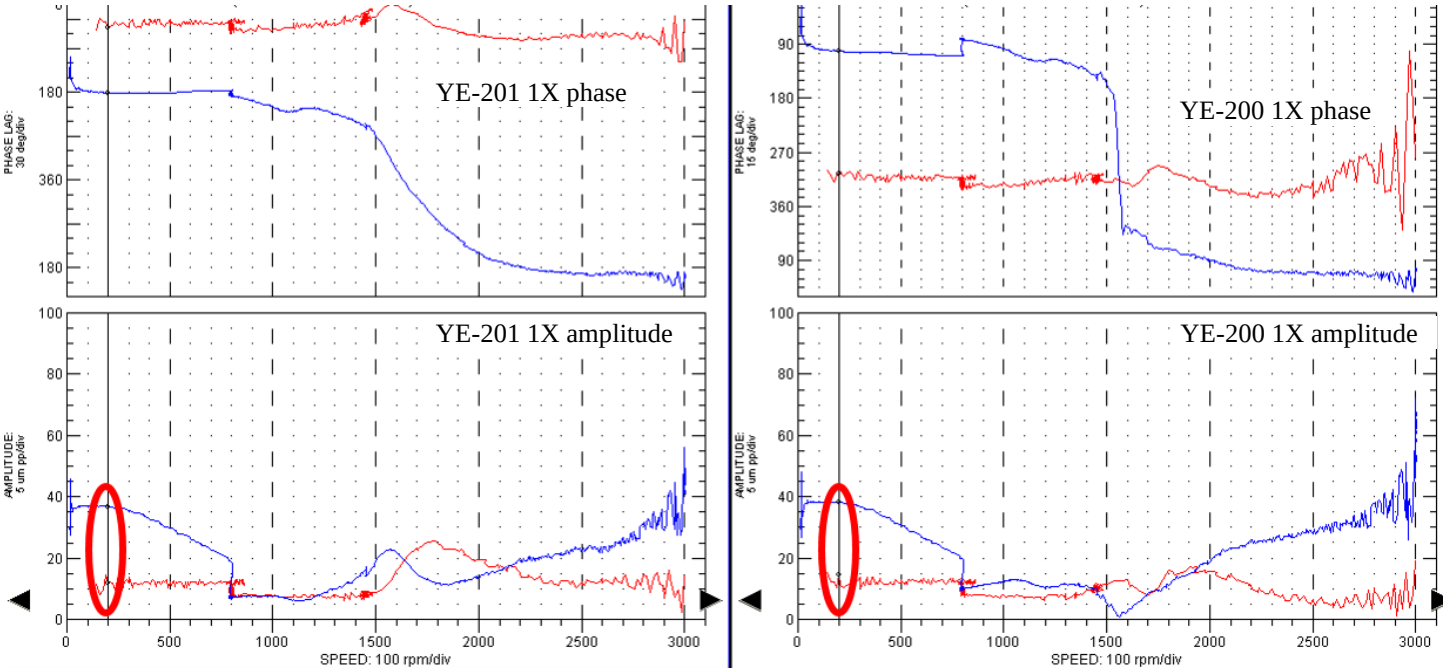

Fig.9. Uncompensated 1X Bode Plots, (Red-June 20, 2008; Blue-July 29, 2009)

The 1X compensated Bode plots (Fig. 10) show the rotor 1st balance resonance frequency shifted to a lower speed (red arrow) during the startup in 2009 (left) when compared to the startup in 2008(right). For the compared startups, the first resonance frequency changed from approximately 1750–1800 rpm to 1550–1620 rpm. A lower resonance speed implies a decrease in the rotor modal stiffness with the normally acceptable assumption that the rotor mass remained unchanged. A decrease in modal stiffness is one of the expected (and primary) symptoms of a rotor crack.

The Synchronous Amplification Factor (SAF) calculations derived from the Half-Power Bandwidth method are shown in the blue square insets in Fig. 10. From the shape of resonances, we can see increase in the SAF. The half-power bandwidth method in this case gives similar results for both runs, because the resonance curve is far from the ideal characteristic (due to split resonance). It should be also noticed that the compensation of year 2008 data (right plot) is not correct. Using the peak ratio method, we can estimate a four times increase in amplification of the response at the resonance A similar change was visible on bearing1 too, not presented here. A decrease in effective damping, as shown in that case, is an indicative symptom of a rotor crack. The red arrow highlights the shift of the critical speed to the left, to a lower speed, due to propagating rotor crack and lowered modal stiffness.

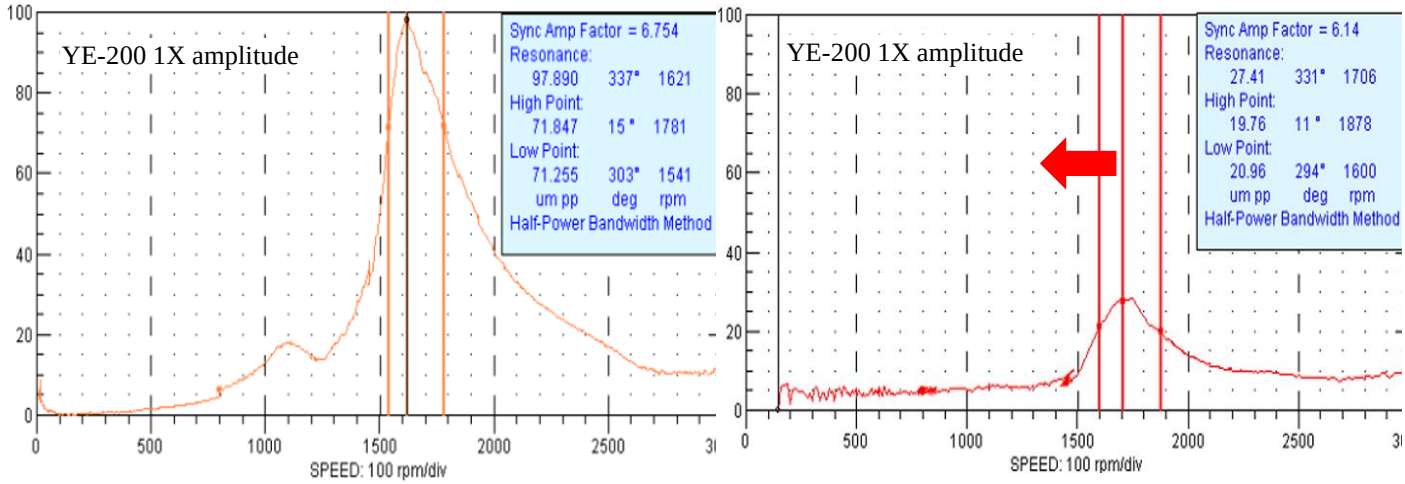

July 29, 2009 June 20, 2008

Fig.10. 1X Bode Plots (compensated on the left and not compensated on the right), Y probes, Half-Power Bandwidth Method at two dates.

The plots in Fig. 11 below compare the startup and shutdown rotor responses recorded on the same day, July 29, 2009. The Bode plots show a significant rise in the slow roll vectors amplitudes during shutdown (blue curves) versus startup (red curves). The amplitude rise from 36 um pp (1.42 mil pp) to 73 um pp (2.87 mil pp) represents a two-fold increase. The increased in amplitude for the 1X slow roll vectors indicates pronounced rotor bow due to crack opening. The phase of the slow roll vectors for startup and shutdown is the same (180°-190°), confirming unidirectional rotor bow in the direction of the deepest crack. The phase (180°) during the shutdown on bearing 1 is almost constant. This is suggesting that rotor crack is fully opened in the 180° direction during the shutdown. Slow roll vector amplitude for the DE bearing 1 is almost six times higher at shut down than in the NDE bearing 2, indicating that crack location is closer to the bearing 1.

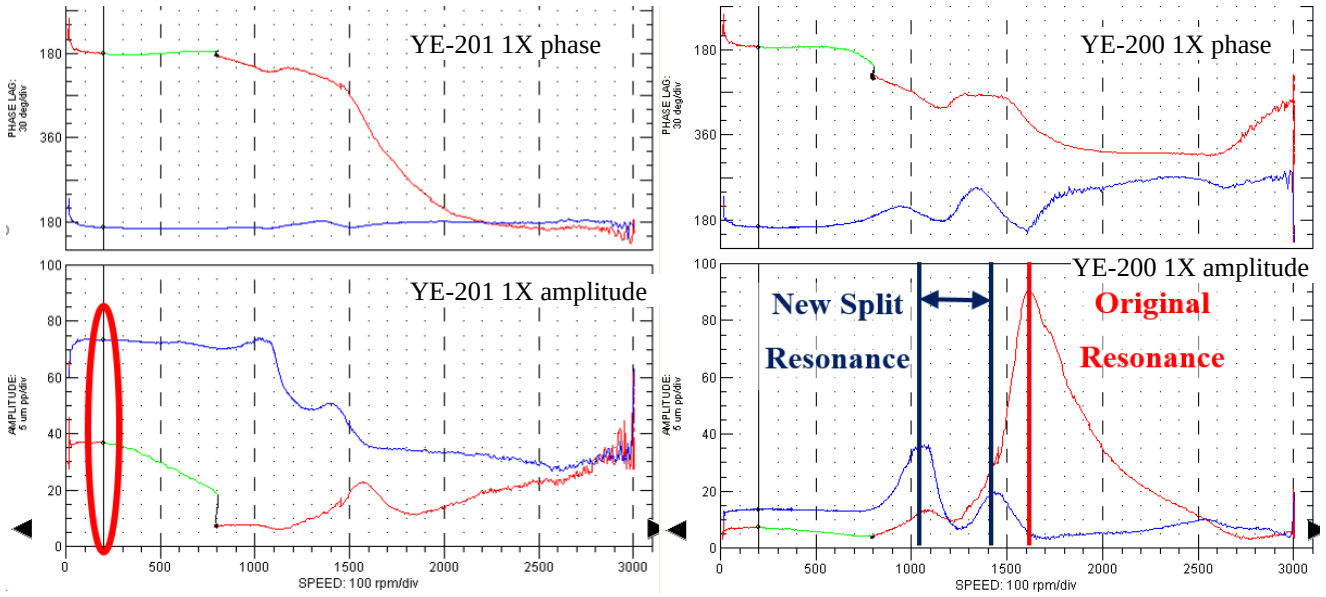

Fig.11. Uncompensated 1X Bode Plots, (Red-start up July 29, 2009; Blue-shut down July 29, 2009)

Conclusion from the data plots with respect to Rule #1:

- Increase in rotor bow demonstrated by changes in slow roll vectors.
- Decrease in modal stiffness demonstrated by a shift in imbalance resonance.
- Decrease in effective damping demonstrated by a higher SAF.

The decrease in rotor stiffness demonstrated by shifted lower balance resonances and the decrease in effective damping demonstrated by higher Synchronous Amplification Factor (SAF) are symptoms of a growing rotor crack.

How does Rule #2 apply?

As per Rule #2, in general, the symptoms of the propagating transverse crack can increase rotor stiffness asymmetry—which likely produces the 2X frequency component—if the rotor is subjected to a steady unidirectional radial load. The 2X component can be greatly amplified when the rotor turns at half (of any) resonance speed because of the excitation of the resonance mode. The above-mentioned symptoms are not visible in our case (see Fig. 12). This can be interpreted as that either there is no crack, or there is not nough radial preload, or that the existing crack does not cause stiffness asymmetry.

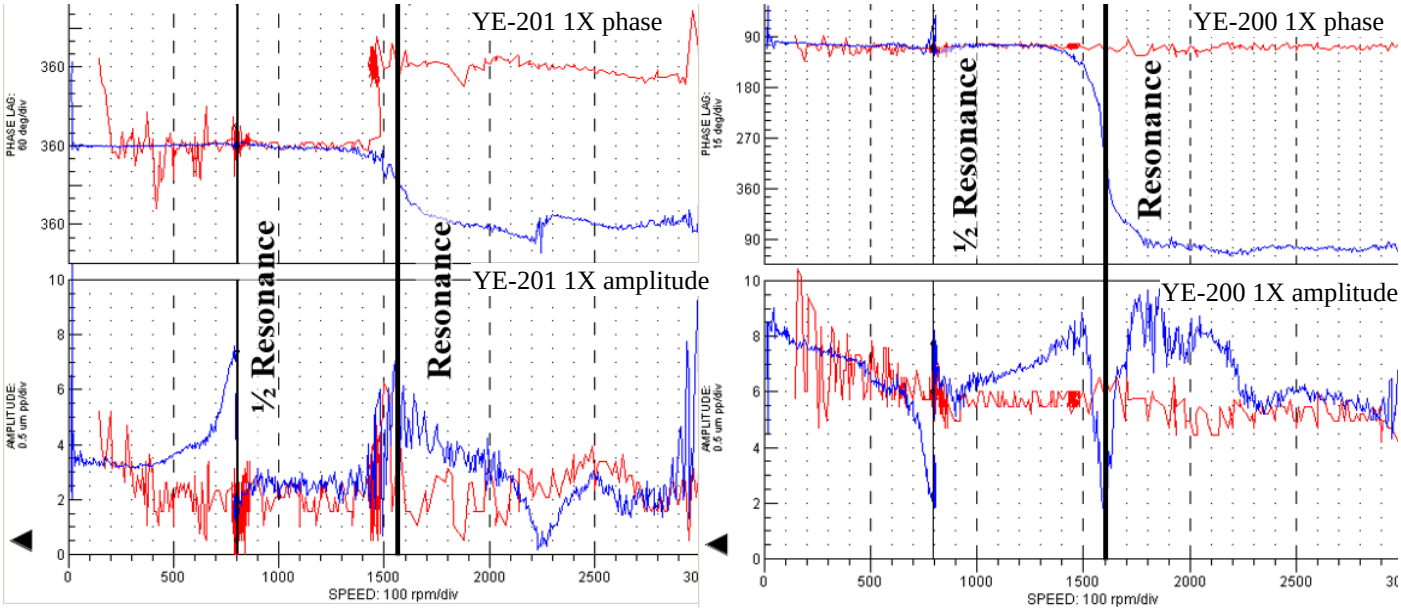

Fig.12. 2X Bode Plots, (Red-June20, 2008; -July29, 2009)

How does Rule #3 apply (thermal sensitivity)?

Each time the rotor heats, there is an apparent temporal change in vibration amplitude, as shown on the Polar plots in Fig.13 . The vibration amplitude is decreasing (orange color) due to initial rotor surface heating and rotor crack closing. Later. as the rotor heats up equally all the way from the rotor surface to the center, the vibration amplitude is increasing (green color) to the previous level and the rotor crack is opening again. This behavior is repeatable as shown on the trend plot in Fig. 14.

The polar plots in Figure 13 show the rotor 1X response change over the same time range and evidence:

- Abnormal unidirectional rotor response
- During rotor heating, the crack closes (orange), the 1X response is decreasing.
- After thermal equalization, the crack opens (green), the 1X response is increasing due to the fact that the bow is increasing.

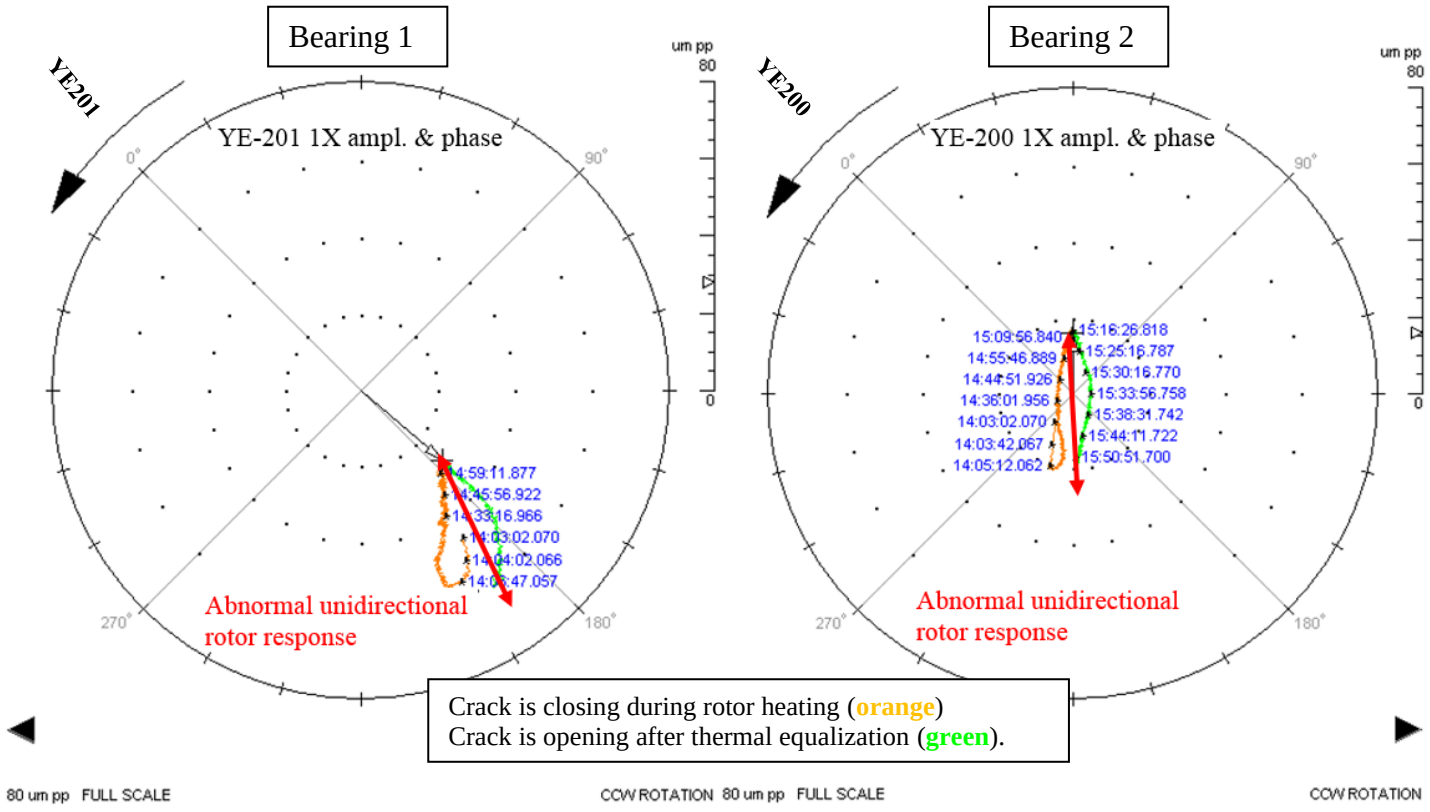

Fig.13. 1X polar plot showing abnormal unidirectional rotor response changes with temperature.

Abnormal unidirectional rotor response change with the temperature change (Fig.13) is another symptom supporting the possible presence of a turbine rotor crack. The change of the shaft relative vibration, always in the same direction, suggest sudden changes in the rotor bow, possibly caused by "closing" and "opening" of the shaft crack.

Polar plots (Fig. 13) for steam turbine DE bearings 1 (left) and NDE bearing 2 (right) show the unidirectional change of the shaft relative vibration during the rotor heating (orange). The change of the shaft relative vibration and eccentricity (pk-pk) measurement, together with phase step changes (in 1–2 minutes), always in the same direction, suggest sudden changes in the rotor bow, possibly caused by „closing" and „opening" of the shaft crack. The Polar plots for bearings 1 and 2 show the unidirectional change of the shaft relative vibration during the rotor heating. As the rotor thermally equalizes, in our case, in one hour after the synchronization (and three hours from startup), the direction of the vibration suddenly changes to the opposite direction (green). The possible explanation of thermal sensitivity for the axially heated rotor is that the transverse crack acts as the insulation. The heat transfer is faster on the opposite side of the crack and the rotor starts to bow in this direction, causing the crack to close (accompanied with a decrease of 1X response) until the temperature equalizes (Fig.7). There are also some models described in the literature for radial heat transfer, concluding that for a transverse crack the heating of the rotor should cause the temporary closing of the crack (the surface of the shaft expands more and faster than the center of the shaft) until the temperature equalizes. The same can be seen on Amplitude and Phase Trend Plot (Fig. 14), where the phase is nearly constant, confirming unidirectional behavior.

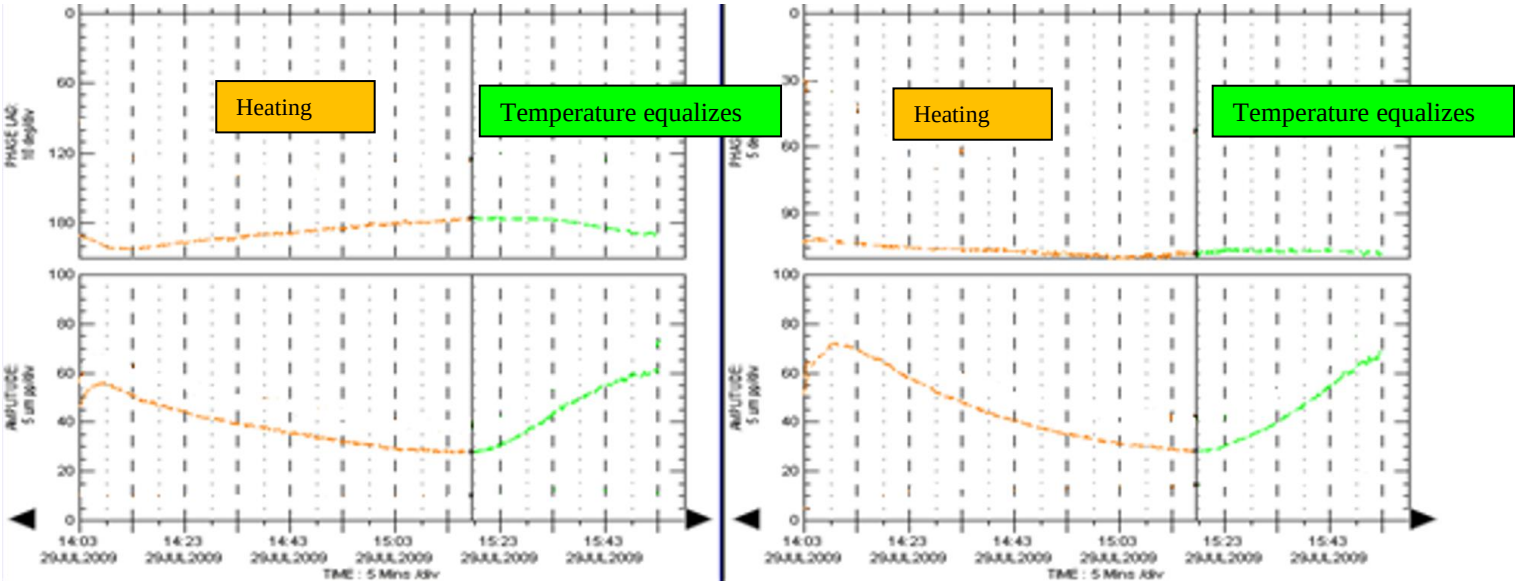

Fig.14. Bearing #1 (DE) Amplitude and Phase Trend Plot

A plausible explanation of thermal sensitivity for the axially heated rotor is that the transverse crack acts as a thermal insulation (layer). The heat transfer is faster on the opposite side of the crack and the rotor starts to bow in this direction, thus causing the crack to close until the temperature equalizes. As described in the literature discussing models for radial heat transfer, with a transverse crack the heating of the rotor should cause a temporary closing of the crack (the surface of the shaft expands more and faster than the center of the shaft) until the temperature equalizes).

Conclusion from the vibration data analysis.

- Decrease in rotor spring stiffness demonstrated by decrease in resonance frequency.
- Decrease in effective damping demonstrated by higher Synchronous Amplification Factor (SAF), see Figs 10 and 11.
- Abnormal rotor thermal and load sensitivity.
- Repeatability of abnormal unidirectional rotor response.
- Changes in rotor properties in time – intensity of symptoms is increasing
- Rules #1 and #3 are verified. Rule #2 does not apply in this case.

Any of the symptoms alone is not certain **proof** of a crack. However, the presence of a crack would explain each of the symptoms.

Steam turbine cracked rotor model results

Previously the cracked rotor was analyzed and the process of rotor crack detection using the vibration measurements described as per Rules #1, #2 and #3. The vibration measurements can give the proof of the rotor crack, along with a precise lateral angular location of the deepest crack and an approximate longitudinal location of the crack. A rotor dynamic model can confirm the longitudinal location of the crack and can define the crack depth. This analysis was used to confirm the results after the crack location and depth were known.

The shaft FEM model of actual steam turbine rotor was designed (Fig. 15) based on the steam turbine manufacturer rotordynamics report containing necessary shaft design information. The shaft model located a circumferential crack at the dovetail groove in the first-stage buckets. The model (or crack) was designed with double-sided conical beam Finite Elements. The smaller diameter beam of the crack section represents the actual shaft material left after the circumferential crack propagation. The crack location section was defined in the dovetail groove, under the first-stage buckets, as found in the actual rotor [9].

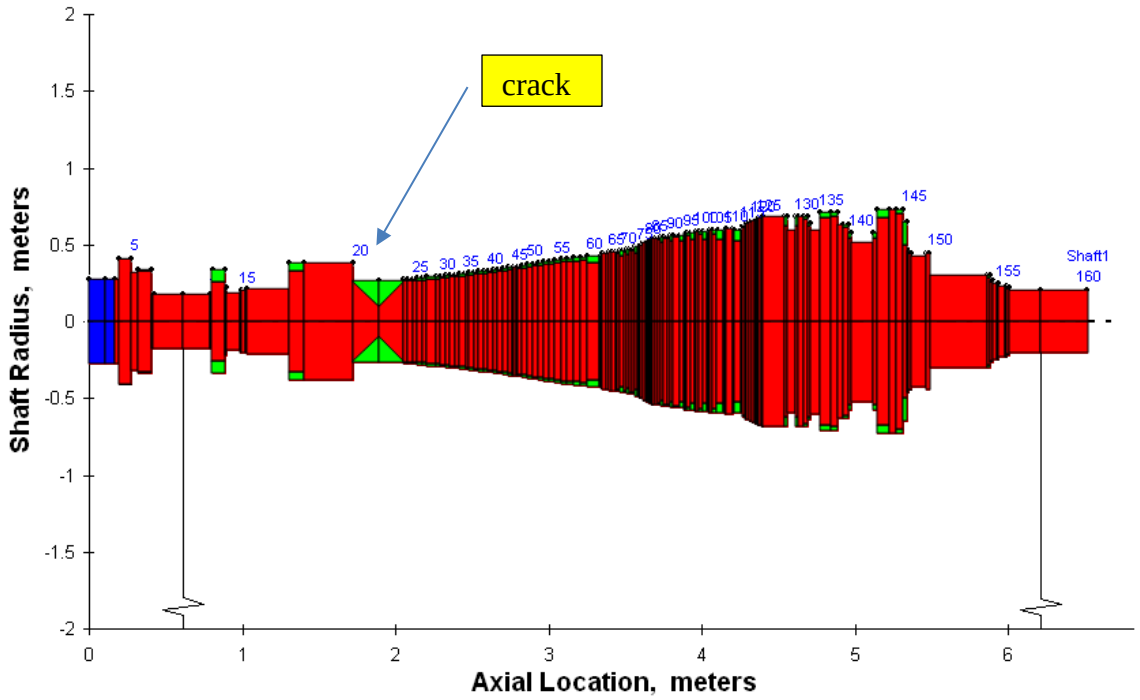

Fig.15. Shaft Model of rotor with a crack.

Running undamped analyses

The undamped critical speed map (Fig. 16) shows the comparison of the natural frequency's changes with the support stiffness for the cracked steam turbine rotor. The unchanged vertical (Kxx) and horizontal (Kyy) stiffness of the bearings is overlapped on the plot. The undamped critical speed of 1305 rpm is estimated for cracked steam turbine rotor for the overlapped bearing stiffness. Comparison of the undamped critical speed (1629 rpm) for the solid steam turbine rotor (Fig. 16a) and undamped critical speed (1305 rpm) for the cracked steam turbine rotor (Fig. 16b) shows a marked decrease in the critical speed for the translation mode (black line). The 1st bending mode (green line) shows an even more significant decrease in natural frequency, from 4,071 rpm for the solid rotor (left), to 2,623 rpm for the cracked rotor (right) at the same bearing stiffness (1 million N/m). This is fully in accordance with the crack detection method described in the first part of Ref. [9] and the decrease in modal stiffness is one of the expected and primary symptoms of a rotor crack.

In general, the first and second natural frequencies (heaving and conical modes) are primarily dependent on support characteristics. These resonance frequencies depend primarily on the bearings' stiffnesses. The crack will influence these rotor modes only slightly. The upper level bending modes (3rd and 4th critical speeds) are heavily dependent on rotor stiffness and are substantially influenced by shaft cracks that degrade the overall rotor stiffness.

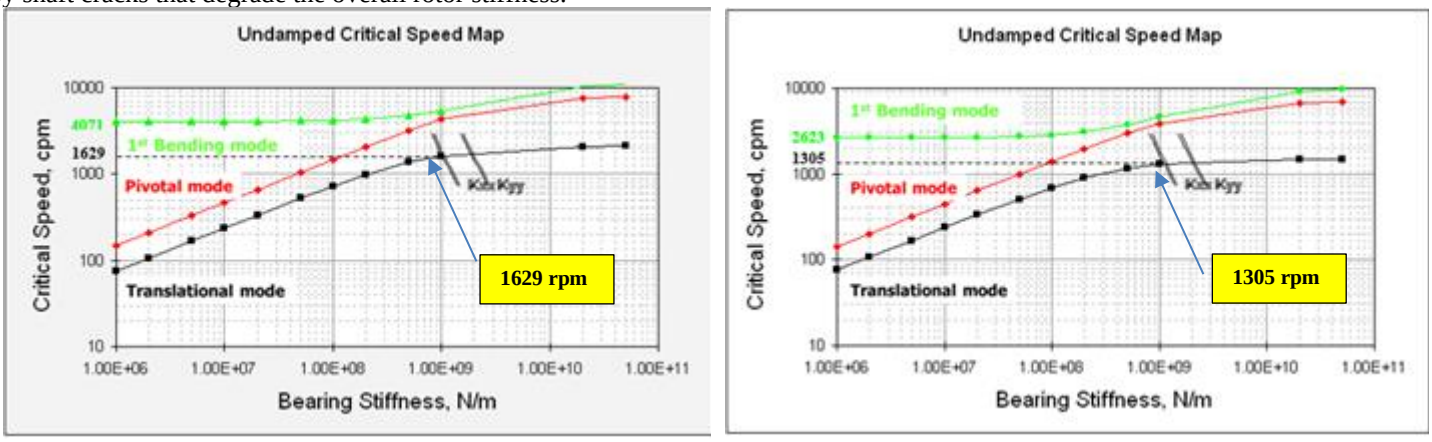

(a) Solid rotor (b) Rotor with crack

Fig.16. Undamped Critical Speed Map for solid turbine rotor (left), for cracked turbine rotor (right) with bearing coefficient at critical speed.

Analyses comparison

Comparison of the undamped mode Shape Plots (Fig.16) for the solid steam turbine rotor (left) and the cracked turbine rotor (right) shows there is visible significant change in the deflected shaft centerline. The deflected shaft centerline (Fig.17) for the cracked rotor is sharply bent at the crack location, closer to the steam turbine DE bearing 1, possibly explaining the crack propagation in the circumferential manner.

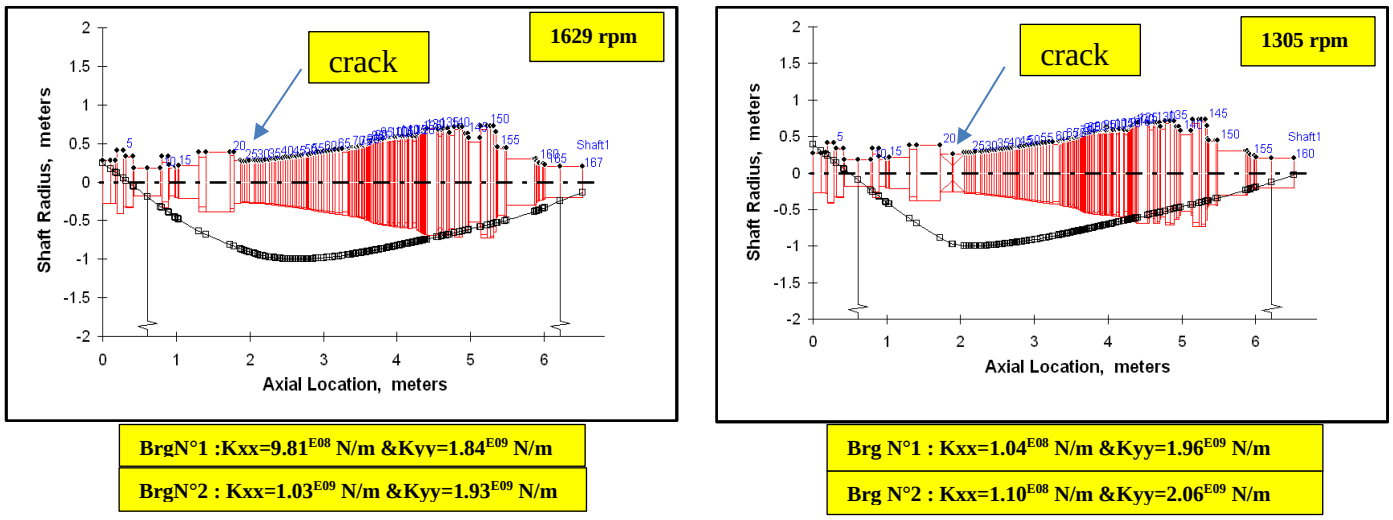

BrgN°1 :Kxx=9.81^{E08} N/m &Kyy=1.84^{E09} N/m

BrgN°2 : Kxx=1.03^{E09} N/m &Kyy=1.93^{E09} N/m

Brg N°1 : Kxx=1.04^{E08} N/m &Kyy=1.96^{E09} N/m

Brg N°2 : Kxx=1.10^{E08} N/m &Kyy=2.06^{E09} N/m

(a) Solid rotor (b) Rotor with crack

Fig. 17. Deflected Shape Plots for solid turbine rotor (left) and cracked turbine rotor (right).

Steam Turbine rotor crack confirmation

Based on the above analysis confirming the rotor crack presence, the rotor was removed from the steam turbine and inspected. An impact hammer test was performed first and a reduced first resonance at 19Hz (1140rpm) was confirmed. The buckets of the steam turbine high pressure section, from stages 1 through 28 were machine to inspect the bottom of the dovetail groove. Due to the assembly procedure for this rotor it is not possible to remove the buckets without damaging them. Because of the costs to de-blade the rotor, Non Destructive Testing (NDT) was not previously performed in the dovetail grooves; however the vibration test results described in this case history were considered sufficient justification to incur the additional costs of de-blading and NDT re-testing.

The rotor transverse crack was confirmed under the first-stage buckets in the dovetail groove, see Fig. 18. The crack was symmetric and 360° in circumferential extent, thus explaining the absence of the 2X frequency component increase.

The crack depth was not possible to obtain as the rotor was taken by the insurance company and all the tests stopped for about one year. This was the reason to continue investigating the rotor crack depth and behavior using the rotor modeling.

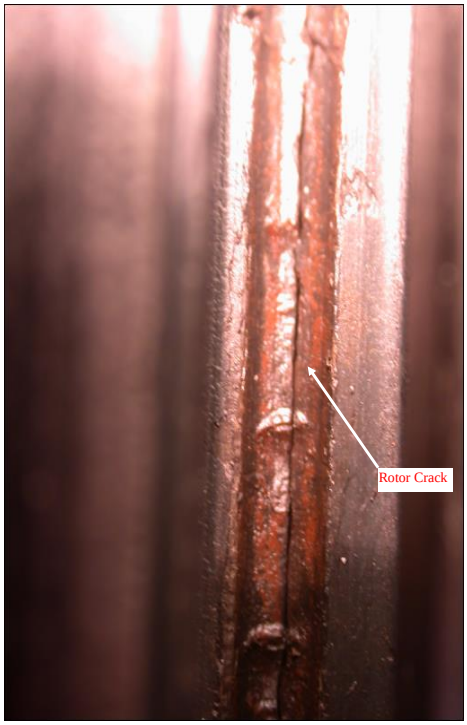

Fig. 18. The steam turbine rotor dovetail groove with circumferential crack

A developed model of a real steam turbine rotor was used to represent the rotor with the same circumferential crack as detected in the actual steam turbine. The validated steam turbine cracked rotor model with a known longitudinal crack location was used for the crack depth estimation.

The steam turbine rotor was later taken out of the machine and cut thru the cracked section (Fig. 19). The picture on the left shows the diameter (0.25m) of uncracked part of the rotor. The uncracked section diameter represents only 50% of the original total shaft diameter. The second picture on the right (Fig. 19) displays the cracked surface area, i.e. total area of cut section without uncracked area. The cracked surface area represents 77% of the total cross sectional surface area.

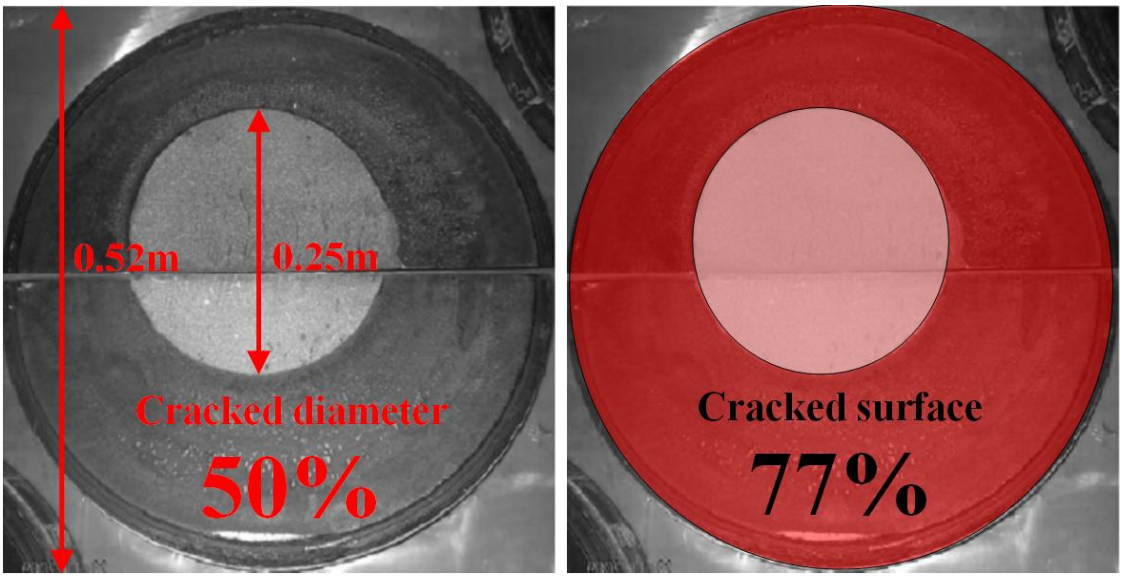

Fig. 19. The steam turbine rotor crack section pictures cracked shaft diameter (left) and cracked surface area (right)

The steam turbine rotor crack section was thoroughly investigated, and the crack depth measured every 15° circumferentially. The measurement results are documented in the table and the sectional drawing shown in Fig. 20. The angles are set with respect to the

YE-201 reference transducer, measured against shaft rotation. The zero is defined according to the phase measurement convention used in the vibration monitoring, i.e. under the YE-201 reference transducer, when the Keyphasor notch on the rotor is aligned with the Keyphasor probe (KPH1).

The biggest crack depth was measured at 210° angular direction (green line), exactly as predicted by the vibration measurement results. The estimated angular direction of the rotor crack was estimated at 190°-210° from YE-201 reference transducer, measured against the rotation.

YE-201 [deg]	depth [mm]
0°	84
15°	80
30°	84
45°	90
60°	99
75°	109
90°	119
105°	128
120°	127
135°	145
150°	152
165°	154
180°	157
195°	160
210°	165
225°	162
240°	154
255°	145
270°	137
285°	130
300°	119
315°	108
330°	197
345°	88

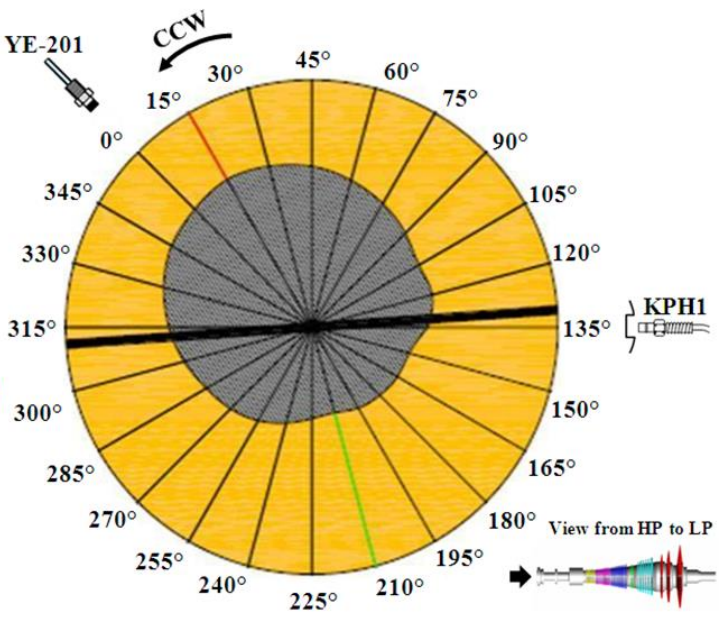

Fig. 20. The steam turbine rotor crack section

SECOND CASE

Introduction

The machine train (Fig 21) consists of a single-shaft heavy duty Gas Turbine (120MW, 3000 rpm) directly coupled on the hot end to a synchronous generator. The compressor portion of the gas turbine rotor consists of stacked blade wheels held with tie-bolts and it is connected to the turbine rotor via a marriage joint. The turbine rotor consists of three turbine wheels with buckets held together with through bolts. The rotor is supported by three main journal bearings (Brg. 1, 2 Elliptical, Brg. 3 tilting pad).

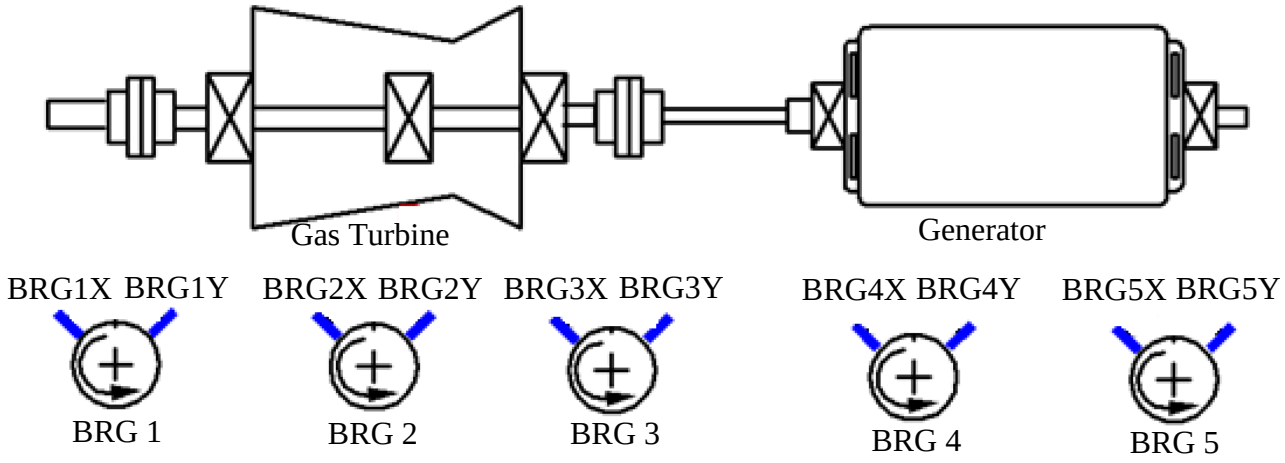

Fig. 21.Machine Train Diagram with the location of vibration transducers.

Discussion of vibration measurements

How does Rule #1 apply ?

The uncompensated 1X Bode plots (Fig 22) show small increase in slow-roll vectors when comparing start-up/shut down 6 and start-up/shut down 7, indicating an increase of rotor bow. There is visible change in the balance resonance frequency between start-up and shut down, decreasing from 2500rpm to 2133rpm, suggesting a decrease in modal stiffness. This abnormal change is repeatable for start-up 6 (SU6) and start-up 7 (SU7). A decrease in modal stiffness is one of the expected and primary symptoms of a rotor crack. Thus, the observed increase of rotor bow demonstrated by changes in slow roll vectors, the decrease in modal stiffness demonstrated by a downward shift in the balance resonance, and the decrease in effective damping demonstrated by the higher amplitude peak at resonance are all indicative of a rotor crack. In addition, repeatability of abnormal rotor behavior is a typical symptom of a cracked rotor.

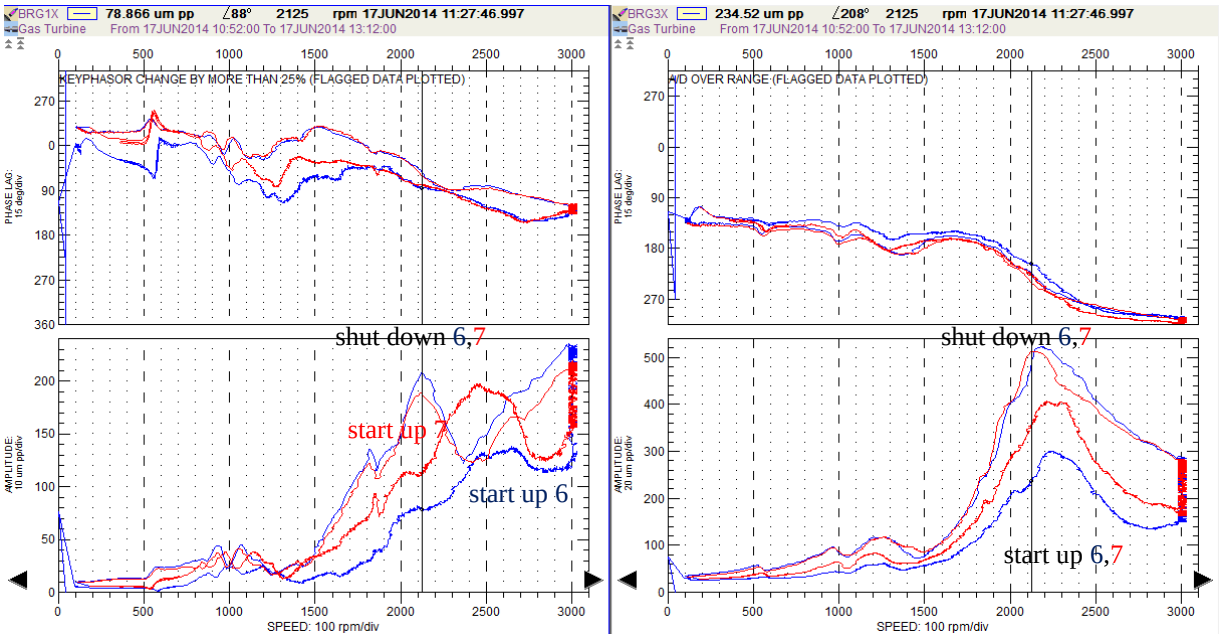

Fig. 22.Uncompensated 1X Bode plot of rotor vibrations for GT brg.1, 3 for SU6 (blue) and SU7 (red).

Repeatable abnormal behavior and same symptoms as described above are visible as well on uncompensated 1X Bode plots (Fig. 23). Visible split resonance during the shutdown not present during the start-up, may suggest the crack propagation. The rotor transverse crack causes stiffness anisotropy in the rotating system and appearance of split resonance.

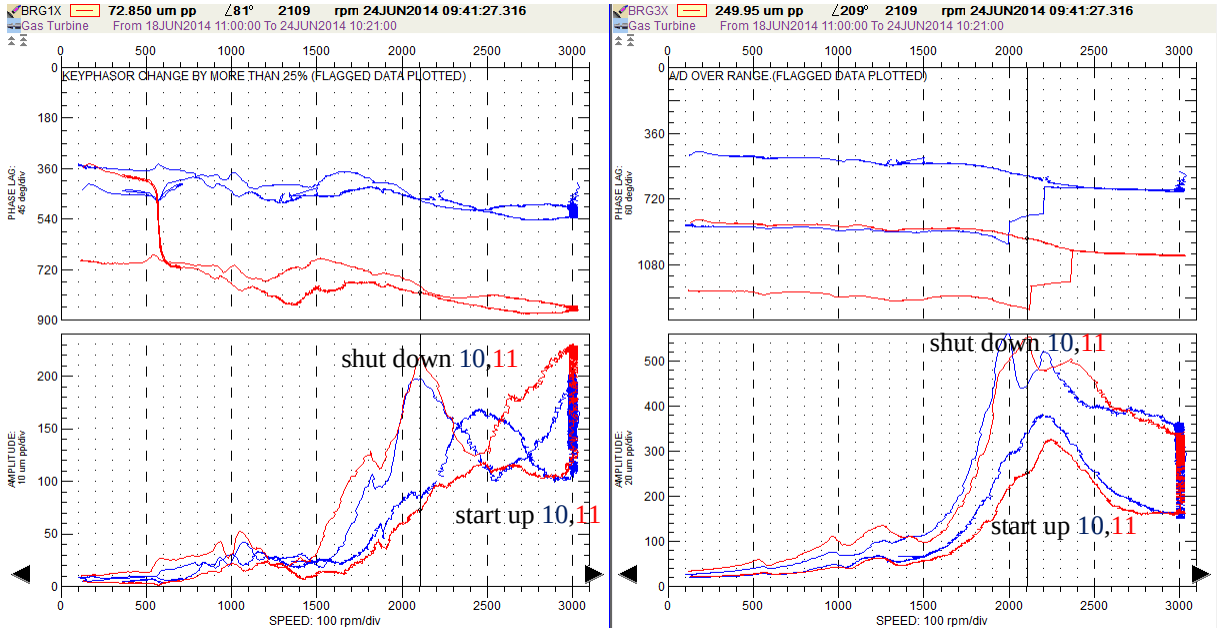

Fig. 23.Uncompensated 1X Bode plot of rotor vibrations for GT brg.1, 3 for SU10 (blue) and SU11 (red).

The 1X polar plots (Fig. 24) show the slow roll vector change between the start-up (SU) 11 and shut down (SD) 11. The resultant red vector shows the unidirectional change, confirming the change in the rotor bow, possibly caused by a rotor crack.

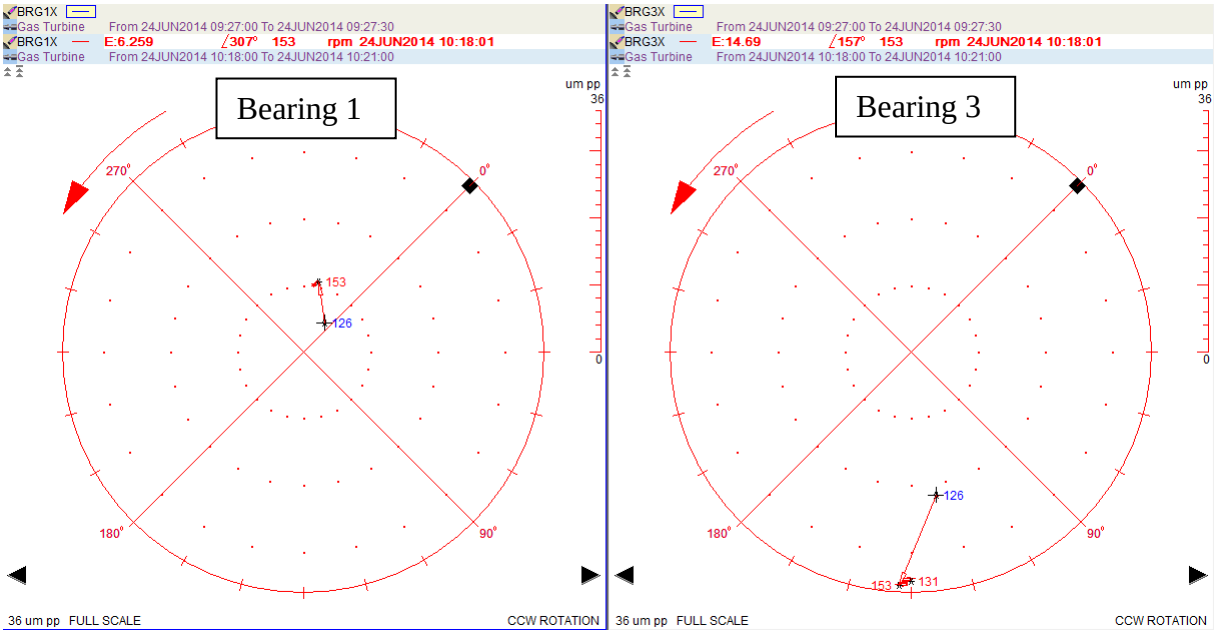

Fig. 24. 1X Polar plot for GT brg. 1, 3 showing slow roll vectors SU11 (blue) and SD11 (red).

Polar plots (Fig. 25) show abnormal unidirectional rotor response change during the steady state conditions. The shaft-relative vibrations increased in one direction, suggesting the rotor bow increased. This suggests that rotor bow was increased due to crack opening and the 1X vibration component was increased due to the modified bow and unbalance. This abnormal rotor behavior is exactly repeatable for start-up 10 (blue) and start-up 11(red). Repeatability of abnormal-unidirectional rotor response is typical sign of rotor crack.

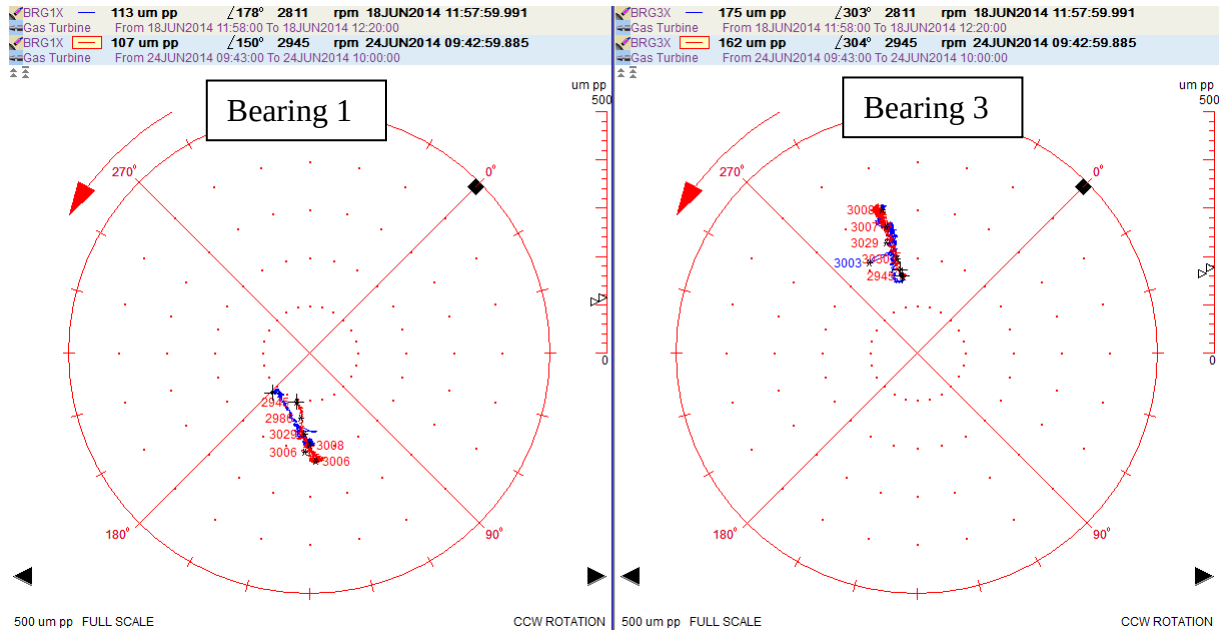

Fig. 25. 1X Polar plot for GT bearing 1 and 3 at steady state SU10 (blue) and SU11 (red).

How does Rule #2 apply ?

In general, a propagating transverse crack can increase rotor stiffness asymmetry, which produces the 2X frequency component if the rotor is subjected to steady unidirectional radial load. The 2X component can be greatly amplified when the rotor operates at half of any balance resonance speed due to excitation of the resonance mode by 2X vibration. The above-mentioned symptom is not greatly visible in our case (Fig. 26).

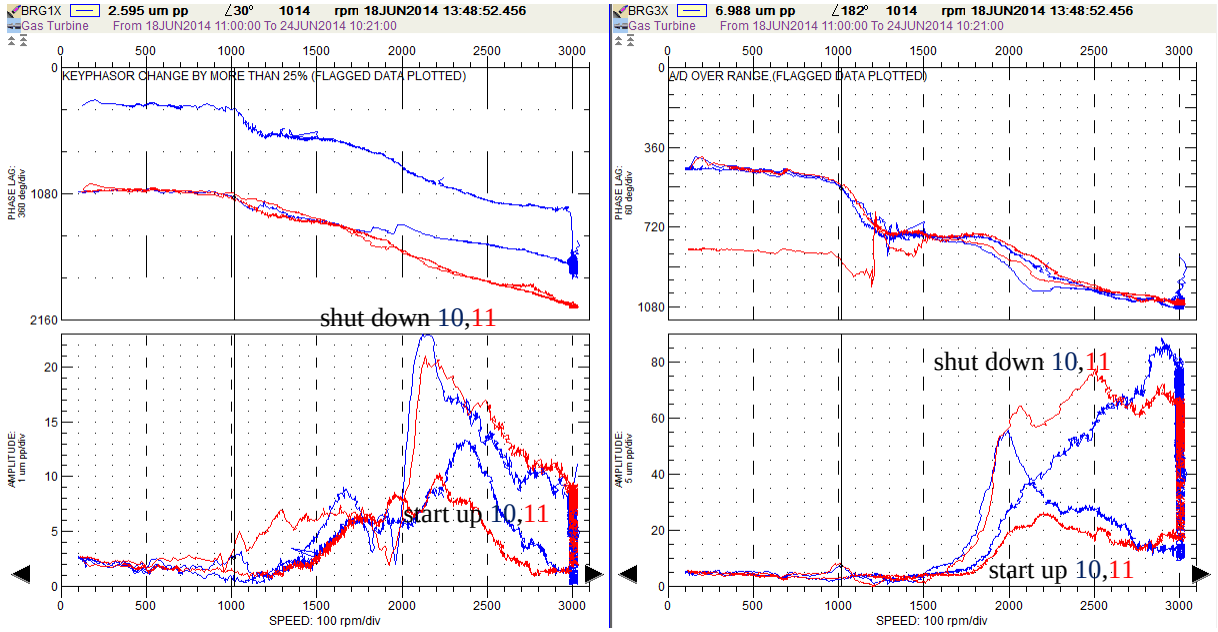

Fig. 26. 2X Bode plot for GT bearing 1 and 3, for SU10 (blue) and SU11 (red).

Conclusion from the vibration data analysis.

Based on the above-stated symptoms, it was concluded that a rotor crack most probably exists on the Gas Turbine rotor. The recommendation was to remove the rotor from the machine and confirm the presence of a crack using the non-destructive testing techniques on the entire rotor. The rotor was removed from the machine and the rotor crack was found at the Turbine forward stub-shaft, at the marriage joint near the bearing 2 (Fig. 27). The crack was 180° circumferential, with variable depth up to 18mm. The absence of significant increase in the 2x frequency component can be possibly explained by lack of radial preload to open the crack, due to vicinity of bearing 2. The case story further showed the difficulty of detecting the rotor crack as primary problem as it can often be masked by other existing machine malfunctions.

The described and detected symptoms of rotor crack in this case were: the increase of rotor bow demonstrated by changes in slow roll vectors, the decrease in modal stiffness demonstrated by shifted balance resonances, the decrease in effective damping demonstrated by higher peak at resonance, the unidirectional changes in the rotor bow, the abnormal rotor behavior and repeatability of abnormal-unidirectional rotor response.

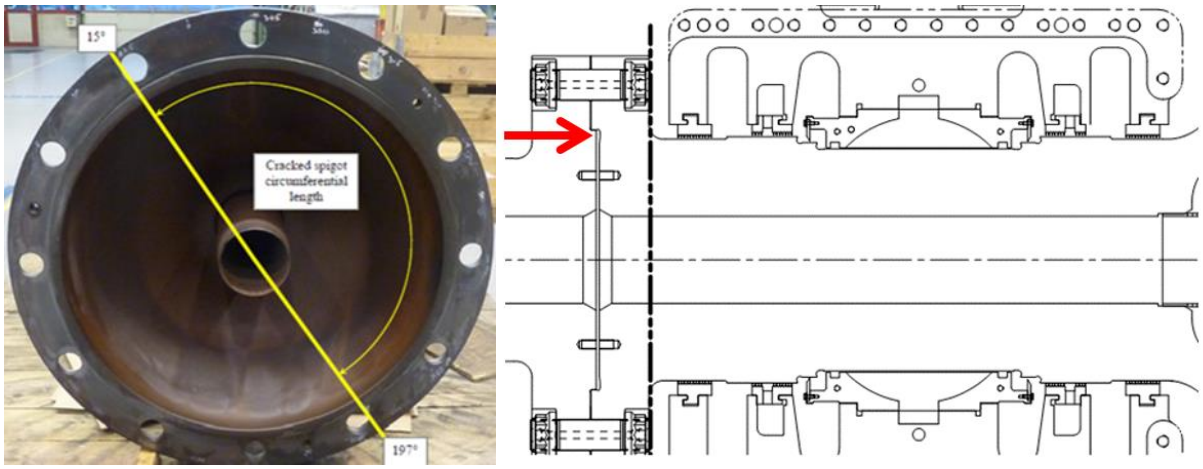

Fig. 27. Rotor crack detected in Turbine near the bearing 2 at the marriage joint.

CONCLUSIONS FROM THE TWO CASES

Looking at the above two cases it can be noted that the second rules (2X vibration) was not present as a signature of a crack.

- For Case #1, the crack was symmetric and 360° circumferential, explaining the absence of the 2X frequency component increase.
- For Case #2, the crack was 180° circumferential, with variable depth up to 18mm. The of a significant increase in the 2x frequency component can be possibly explained by lack of radial preload to open the crack, due to vicinity of bearing 2.
- For Case #1, rules #1 and #3 were present for 1X activity of a cracked rotor response.
- For Case 2, rules #1 was present for 1X activity of a cracked rotor response.

PART II. FLUID INDUCED INSTABILITY

While a shaft crack is probably the most prominent representative of a forced vibration problem, a fluid film induced instability is an outspoken and infamous representative of self-excited vibration phenomena in rotating machinery. Its career started with whirl and whip description by B.L Newkirk in the early 1920's and there are many ways the topic can be presented. The authors were educated by, and teach to the next generations of machinery diagnosticians, the methodology developed by Bently Rotor Dynamics Research Corporation, described for instance in Ref. [1].

A self-excited vibration occurs when a system has a method of converting a non-vibrating energy source to vibration energy. The self-excited vibration takes place at a natural frequency of the system, i.e. at resonance although not necessarily the same resonance we are observing during transient of the machine. In the case of a fluid-induced instability the mechanism is that rotation of the rotor is accelerating the viscous fluid (oil in the bearing, gas or fluid in the seal, any situation where there is fluid in the clearance between rotating and stationary part) and the developed wave of fluid starts to carry the rotor around the clearance. So, for instance in the case of the oil whirl/oil whip instability condition the shaft is no longer operating with the stable position in the presence of the "oil wedge" (a nickname for the pressure profile developed) but the one starts "a wave traveling around the shaft in the bearing clearance, the shaft riding in the bottom of the wave and being pushed ahead by the wave, like a surfboard", to quote John Sohre [12].

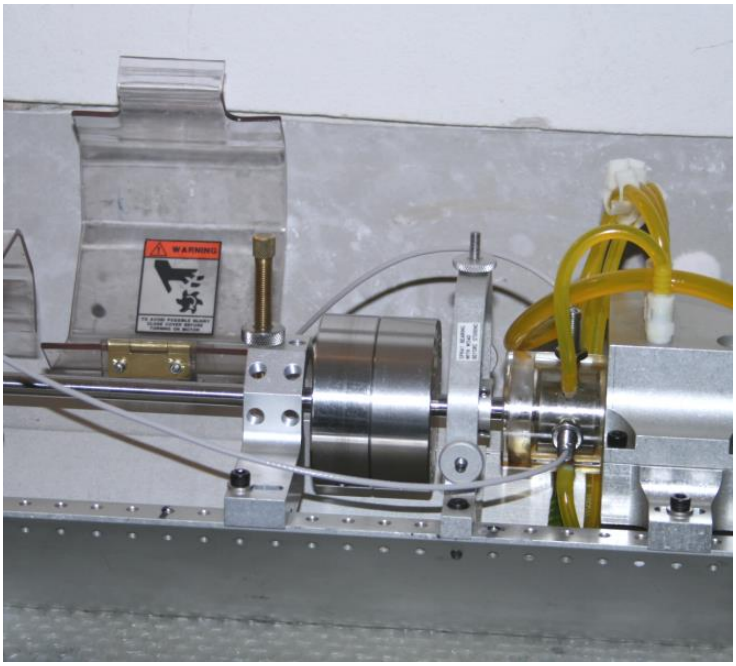

Fig. 28. Oversized, unloaded fluid bearing used in demonstration of fluid induced instability.

When teaching new diagnostics students, the organization the authors are employed uses the test rotor kit with an unstable (oversized, poorly loaded) oil bearing (Fig. 28). Demonstration is aimed to show fluid induced instability characteristics:
high amplitude of vibration, dominated by a forward precession, sub-synchronous component (Fig. 29), circular shape of the orbit with characteristic multiple keyphasor dots (Fig. 30) and average shaft centerline position in the center of the clearance (Fig. 31).

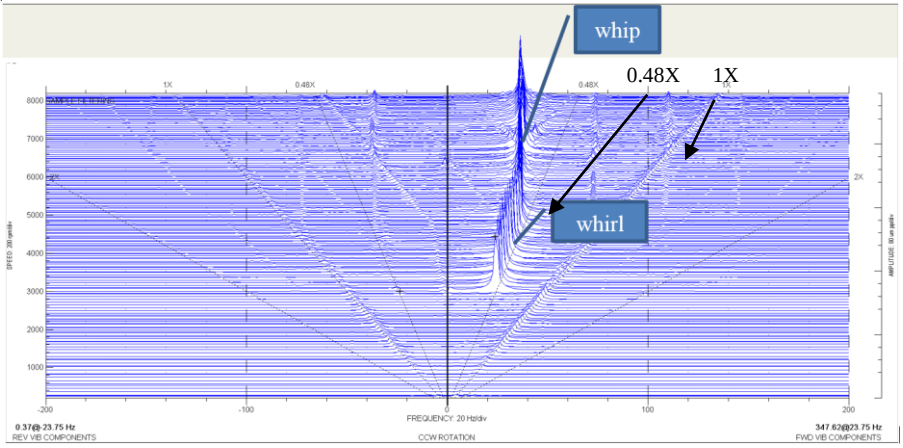

Fig. 29. Demonstration result: forward precession, subsynchronous component vibration for whirl and whip mode.

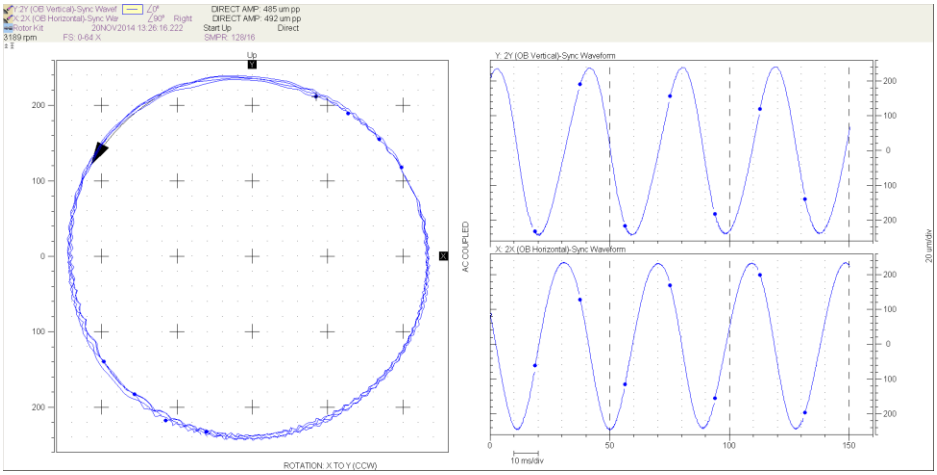

Fig. 30. Sample orbit for instable condition (whirl), with characteristic multiple Keyphasor dots pattern.

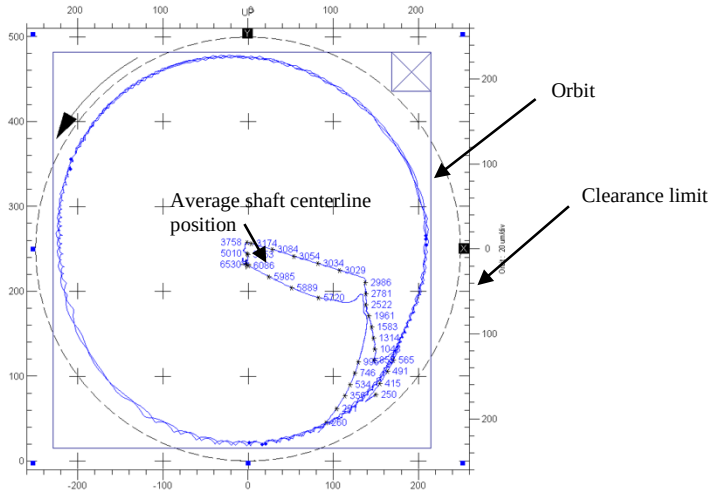

Fig. 31. Shaft centerline plot with an overlay of the orbit in instability condition – orbit follows the clearance, so the average position of journal is at the center of the clearance.

Another important outcome of the presentation is to show the difference between whirl mode, visible in Fig. 29 as the area when the subsynchronous vibration frequency follows the change of rotating frequency at a constant ratio, and whip mode when the vibration frequency is locked at the natural frequency of the rotor.

The explanation involves the model of rotor response [1] that is developed in the training mentioned above in the form of Equation (1): (1)

$$Ae^{j\alpha} = \frac{mr_u\omega^2 e^{j\beta}}{[K - M\omega^2 + jD(\omega - \lambda\Omega)]}$$

where:

A - amplitude of response vector [m]

α – phase lag of response vector

j – imaginary unit, $\sqrt{-1}$

m, r_u, β, ω – defines perturbation by unbalanced mass m [kg] at radius r_u [m] and position angle β rotating with any frequency ω [s^{-1}] (the perturbation frequency)

K – spring stiffness constant, stiffness in radial direction involving rotor stiffness and bearing stiffness [N/m]

M - rotor mass (modal mass) [kg]

D – damping constant $\left[\frac{N\,s}{m}\right]$

Ω - shaft rotative speed [s^{-1}]

λ - fluid circumferential average velocity ratio

Lambda (λ) describes the fluid circulation and this concept plays an important role in the explanation of the fluid induced vibration phenomena, but it is specific to educational model used. By definition, lambda is average speed of the fluid in the clearance (Fig. 32), calculated as a ratio of shaft rotational speed. Consider for example flow of oil through the oil wedge in the bearing: because the fluid is viscous the particles at the bearing surface have the speed ratio of 0 and the ones at the journal surface have the speed ratio of 1, the average is expected to be around ½. Taking into account that there are some losses, part of the oil escapes axially, the lambda for the test bearing is expected to be ~0.48, for normal operating condition.

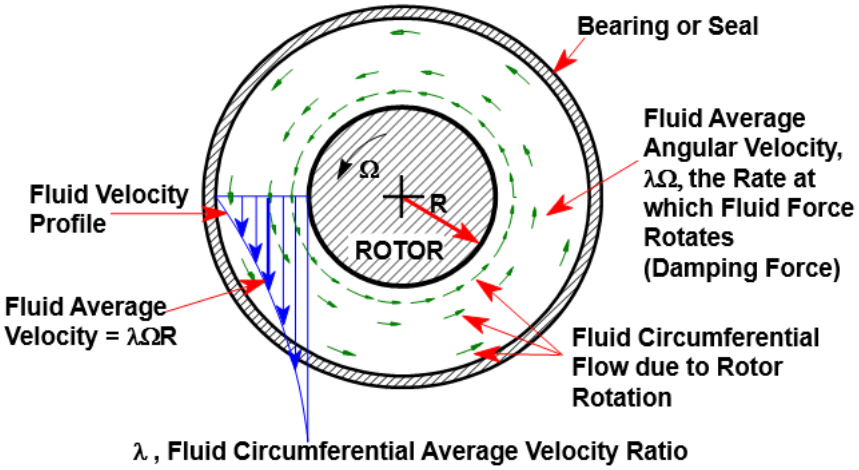

Fig. 32. The concept of fluid average velocity ration, λ

Introduction of λ allows the use of a simple educational model, in opposition to computational models allowing better representation of bearing design, but at the cost of being not-intuitive i.e. requiring numerical calculations. For instance, in the case of a cylindrical bearing, lambda can be expressed [13] in terms of classical bearing (or seal) stiffness K and damping C parameters as (2):

(2) Average velocity ratio, expressed in terms of classic stiffness and damping coefficients

$$\lambda = \frac{K_{xy} - K_{yx}}{\Omega\left(C_{xx} + C_{yy}\right)}$$

So, in the educational model (1) the unstable condition is described by the situation when the term in the denominator, called dynamic stiffness, zeroes. As a result, the amplitude of the response increases to infinity for any non-zero perturbation force in the numerator. The condition of zeroing the numerator requires that both real and imaginary terms equal zero (3,4), at the same time.

Instability condition:

(3) Real part zeroing condition.

$$K - M\omega^2 = 0$$

and

(4) Imaginary part zeroing condition.

$$\omega - \lambda\Omega = 0$$

So, instability can be described as the situation when the rotor is operating (in the bearing or in the seal), at the same time in mechanical resonance (d) and in fluid resonance (e).

(5) Mechanical resonance condition:

$$\omega = \sqrt{\frac{K}{M}}$$

and

(6) Fluid resonance condition:

$$\omega = \lambda\Omega$$

In the whirl mode the fulfillment of the condition (6) is straightforward but the mechanical resonance (5) is the resonance of the rotor mass on the low stiffness spring created by low reaction forces in a poorly loaded bearing. The rotor moves around the clearance as a

rigid body and the reaction forces are low.
For the whip condition, the mechanical resonance condition is easy to see, as the frequency is locked at the rotor natural frequency but to keep the system in fluid resonance the average velocity of the fluid must decrease proportionally to rotor speed increase. The reduction of λ is caused by an increase in vibration and dynamically loading the bearing, thereby reducing the average gap the rotating fluid flows through. The rotor is operating in the bending mode, with all the consequences of increased amplitude at the midspan and the bending stress. The type instability mode (whirl or whip) of the rotor at given condition is governed by the relation of the bearing stiffness K_B and rotor stiffness K_S, acting in a row to constitute spring stiffness K (Fig. 33).

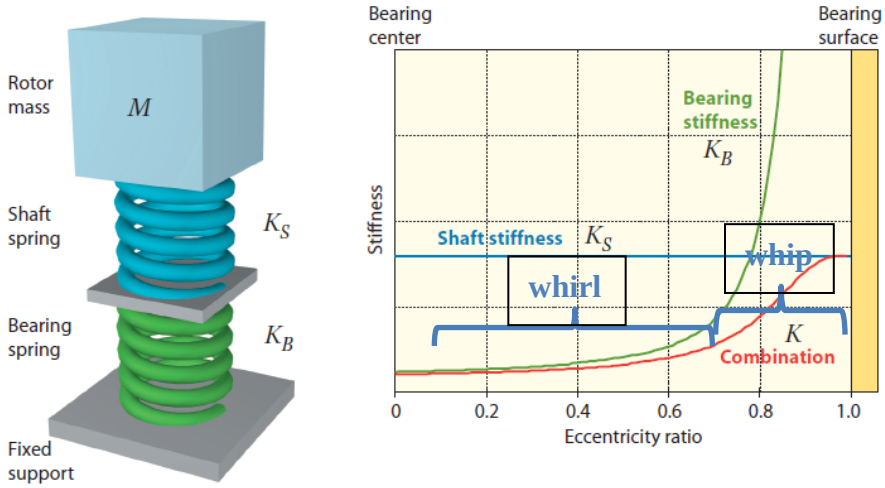

Fig. 33. The whip and whirl areas are depending on the direct stiffness which is combination of shaft stiffness (constant) and bearing stiffness (function of eccentricity ratio).

The educational model allows to teach also other rotodynamic concepts in simple way, for instance stability threshold (7) will be the lowest rotating speed at which instability occurs, calculated directly from (3,4).

(1) Stability threshold:

$$\Omega_{th} = \frac{1}{\lambda}\sqrt{\frac{K}{M}}$$

To stabilize machine i.e. to raise the stability threshold above operating speed we have to increase K, reduce λ, or both.
Additionally, the margin of stability can be introduced as the difference between the frequency of the fluid resonance and the one of mechanical resonance, for a given operating condition.

One more tool used in the diagnosing of instabilities is subsynchronous vibration phase analysis [14], based on the claim that phase lag (measured with transducers of the same angular location) increases as we move further from the source of instability. This is often demonstrated using the above mentioned rotor kit. Tests show phase lag from a few degrees for the whirl condition to almost 90 degrees in case of the whip condition. Note however, that the rotor kit is equipped with only one bearing that can be unstable, the other one (rubber ring supported sleeve bearing) is always producing damping. Based on experience, the results are usually different in the case of real machines, where multiple bearings can become unstable – this will be covered in more details later in the text.

As a result of this training, the diagnostic engineer is equipped with a set of symptoms allowing the identification of fluid induced instability and the selection of cures. Fluid induced instability vibration signal characteristics:

- **Rotor Whirl Frequency is Nearly 0.5X.**
- **Whip Frequency is Asymptotic to Resonant Frequency (="Nameplate", "Critical Speed").**
- **Precession is Always Forward.**
- **Orbit Shape is Circular, or Nearly Circular.**
- **Phase Response, Measured at Points Increasingly Further from the Instability Source, Along the Rotor, Shows Increasing Phase Lag.**

And methods to stabilize machine:

- **Increase K**
- **Decrease λ**

The latter is expanded into practical examples of methods of ensuring machine stability:

- Aligning machine to correctly load the bearing
- Reducing bearing clearance or bearing length
- Using a bearing with more complex geometry (offset-cylindrical, pressure dam, elliptical, multi-lobe, tilting pad…)
- Use of anti-swirl, shunt holes, swirl breakers in seals, application of honeycomb or brush seal and other can be explained through their effect on K, λ, or both.

The practical toolset works, in most cases, so well that diagnostic engineers educated in it are somehow shocked when a machine "refuses" to follow the above rules. Let's analyze some cases to point to limitations of the model but also to prove that with proper review of assumptions it can still be useful in identification and solving the problem.

The first case we review is a barrel type hydrogen compressor, running 10.8 krpm, with elliptical bearings. The Unit developed unstable vibration conditions following an overhaul. When the diagnostic services were called for intervention the unit was already in operation for 5 months and during the entirety of this time it was in a condition of instability. Vibrations were characterized by elliptical orbits with amplitudes at the level of the bearing clearance, forward in precession and with the subsynchronous frequency ~0.44X (Fig. 34). The unit was not equipped with a keyphasor, so there is no multiple dot pattern visible in the orbits.

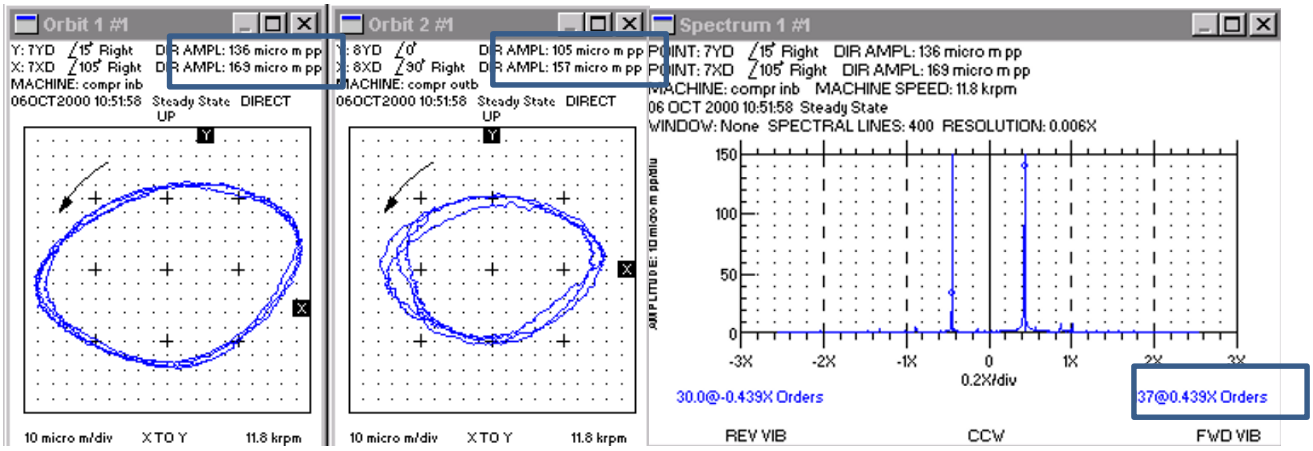

Fig. 34. Fluid induced instability in hydrogen compressor: orbits in both bearings and the full spectrum for bearing 7(DE).

Reason for instability was excessive clearance in brg 7, which can be spotted in the data once the nominal clearances (identical for both bearings) are known – the orbit in brg 7 is bigger than the maximum bearing clearance. During the overhaul the rotor was machined to remove scratches on the measurement path, but the bearing was not changed. The End User was aware about instability as well as the root-cause of it but tried to stabilize the machine when in operation. Furthermore, the operations manager had a constraint on production – a stop of the machine for more than 6 hours would cause long term break of production due to subsequent damages in other machines in the process. The question was which instability: whip or whirl type. The diagnostic engineer claimed it to be whirl, based on the low absolute vibration measured on the bearing covers. Still, the continuation of operation was considered unsafe, in the longer perspective. A new bearing with the bore reduced to match the machined journal was manufactured and the mechanical team was given time to practice the replacement operation on a similar unit in the overhaul. After this training practice, the mechanical team replaced bearing during a short outage window (<5 h). During the shutdown the resonance frequency was confirmed to be higher than 5000 rpm, so the condition was whirl.

Take home messages: 1) - if the machine was stable in the past you can make it stable again (assuming the operating conditions have not changed) by restoring to a nominal condition (bearing clearance in this case); 2) - whirl condition (rigid body motion) is not so destructive as whip. In spite of almost 6 months of operation with unstable vibration conditions, the compressor was not damaged. (Please note - we cannot promise your machine to have same results, so please do not try this at home…)

The first described case was simple because the cause of the instability was known, but in general case the correct identification of location is of critical importance. An 11 MW steam turbine (backup pressure, heat and power generation, 3000 rpm) has never been able to reach full load, even since commissioning 30 years earlier. Previously, several companies were proposing more stable bearings: front bearing was replaced by tilting pad and then replaced again by a "hyper-elliptical" one, with vertical clearance ~0.1% and horizontal clearance ~0.6% of the journal diameter. Diagnostic service was called for evaluation of the machine as it was still unstable for loads >

55% of nominal one (~6 MW).

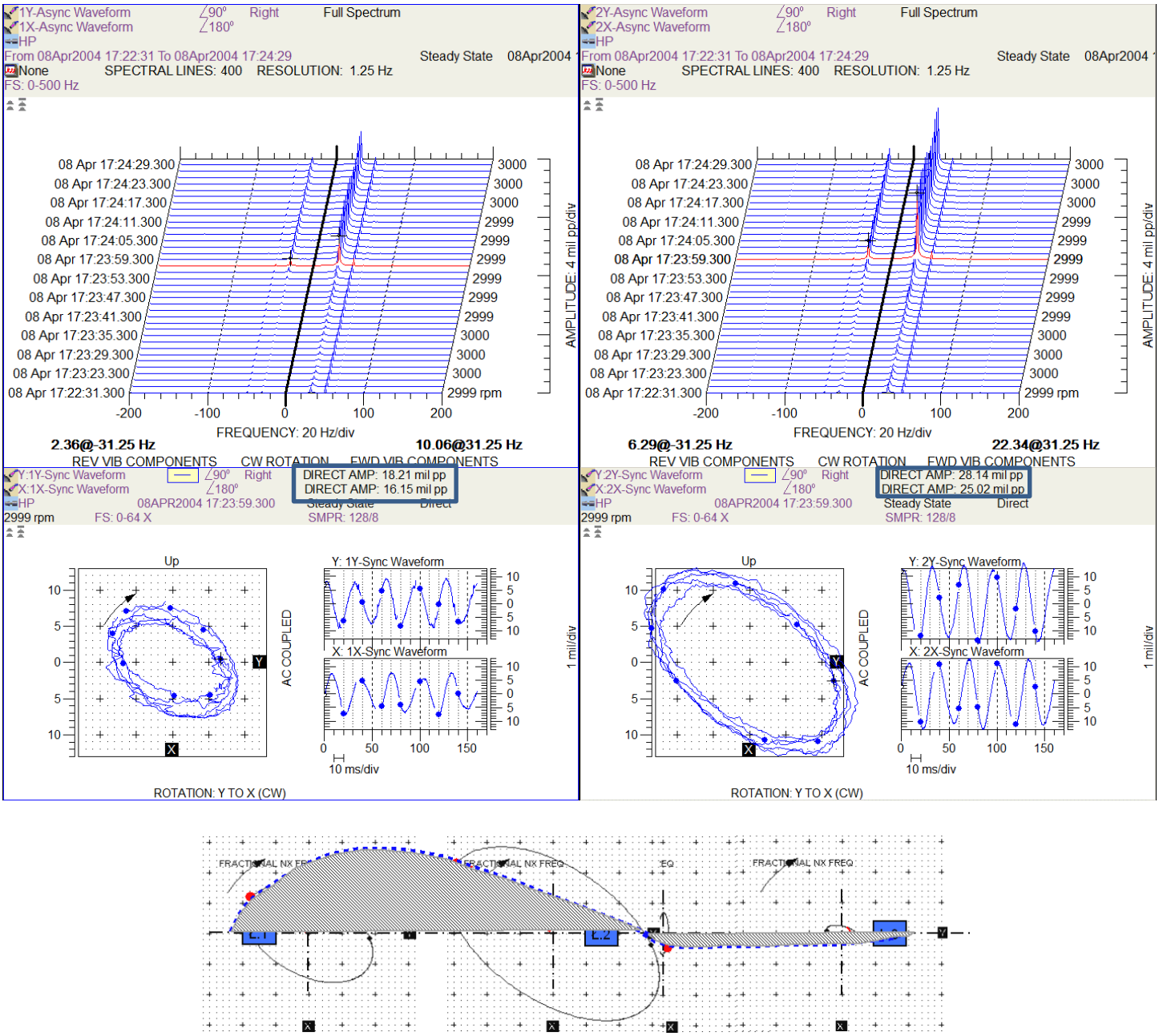

Fig. 35. Unstable operation in HP turbine bearings on inlet steam flow increase: full spectrum waterfall and orbits for bearings 1 and 2, estimated shape of the vibration mode based on orbits measured in bearings 1-3.

The unit was equipped with temporary system to measure shaft relative and casing absolute vibration. The shaft vibrations (because of damaged shaft surface in seal areas) were measured at some distance (up to 10 inches) from bearings (Recommendation is to be 6 no more than 6 inches from the bearing). When the steam flow was increased above threshold ~6MW, the unit developed instability: elliptical shape orbits with forward precession, subsynchronous vibration. The measured amplitudes were significantly bigger than the bearing clearance (up to 29 mil pp vibration amplitude vs. 10 mils vertical and 28 mils horizontal clearance of bearing 2). The frequency coincided with the 1st mode resonance of the rotor, so that was a whip condition.

Due to the orientation of the orbits were not following the bearing clearance, but their axis was rotated, as well as the reaction of the vibration from increased steam flow (to destabilize and to stabilize machine); the steam whip in the long labyrinth seal was hypothesized. In an attempt to track the location, phase analysis was used. The original method brings rather inconclusive result (Fig. 36), which bearing vibration is leading – the leading or lagging is seen differently when X or Y transducers are used.

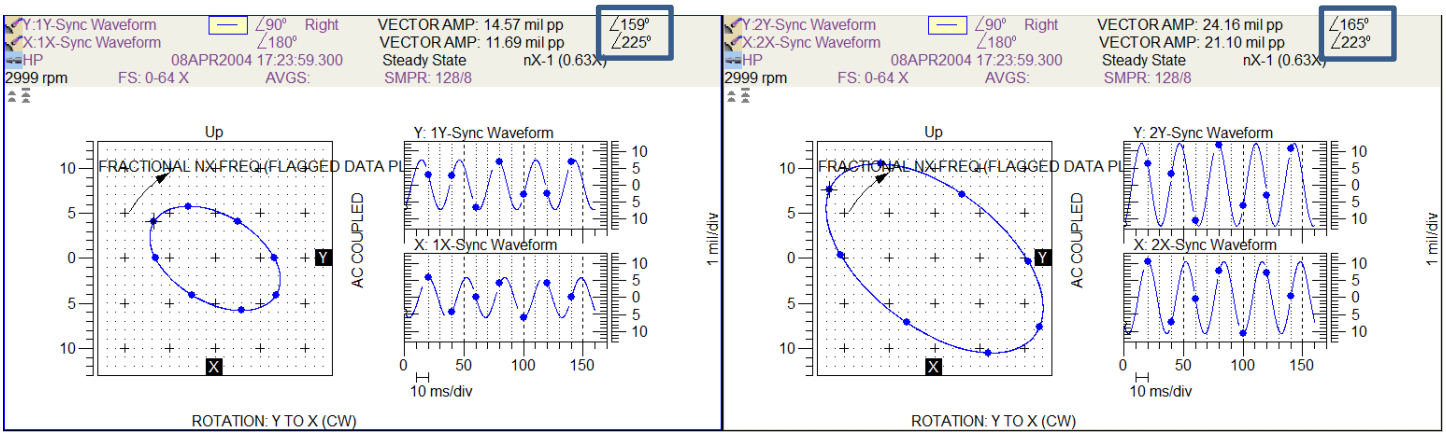

Fig. 36. Orbits filtered to instability frequency: for Y direction bearing 1 leads bearing 2 by 6°, for X direction bearing 2 leads bearing 1 by 2°.

The reason for this inconsistency is the elliptical shape of the orbit, the velocity of the center of the shaft changes as the shaft center moves on its trajectory. To compensate for this error the forward filtering can be used (Fig. 37), a method that was originally developed to compensate for 1X phase error for balance purposes.

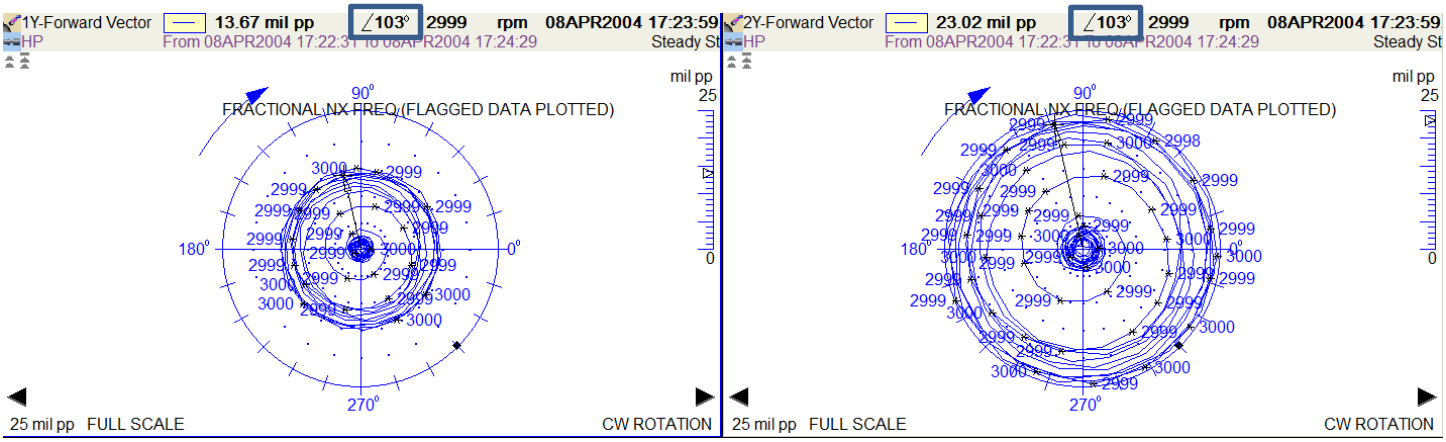

Fig. 37. Polar plot for subsynchronous component, the forward filtered vectors are in phase for bearings 1 and 2.

With this improved method of tracking the phase, there is no lag in motion between bearings 1 and 2. This can be interpreted as the situation when the source of instability is in the middle of span between the bearings but in fact such an interpretation is not always correct. The basis for the phase tracking method is the assumption that the phase lag is caused by the presence of damping. But with a fully developed instability the damping "disappears" i.e. damping forces created because rotor is vibrating in the fluid are counteracted by forces developed by the wave of the fluid that is pushing on the rotor. If one of the bearings is still acting to stabilize the rotor or if there is additional source of damping between source and bearing (consider for instance rub) a delay may be observed, otherwise, the vibrations are in phase. Since damping in the steel rotor is very low compared to normal damping in the bearings it is not measurable by the phase lag in a typical setup, therefore the lag in practice is zero, no matter which seal inside the casing is source of the instability.

The conclusion was that hyper elliptical bearing had failed to improve the stability of the system but the source of the instability was likely between the bearings. Recommendation was made to perform model calculations for stability study and to check feasibility of more stable seals (using swirl breaker, shunt holes, honeycomb seals). Calculation proved the unit to be unstable by original design (for nominal parameters) but due to economic reasons (considering it was a 30 years old machine) it was not modernized and soon scrapped. Interesting comment came from the operators that recalled that in the past there was an attempt to run the unit in unstable condition to "pass the unstable region". Note that the unit was equipped with casing vibration only, no automatic protection, so the shaft vibration levels were not available which can be seen as some excuse for the decision made. As the result of ~20 minutes operation, a large steam leak developed, so the machine was taken off production and inspection revealed complete damage of all labyrinth seals in the HP casing. Considering the levels of shaft vibration observed during the test this history can be readily understood.

The learning from this case can be: 1)- It is not always the bearing that is source of the instability; 2)- It is worth to test solution numerically (model) before implementing it on machine, and 3)- Whip condition is destructive. Do not allow operation in unstable

condition. Preferably - use automatic protection (trip) based on shaft vibration levels.

It is recognized that tilting pad bearings may be an insufficient means to stabilize the rotor, if the source of instability is in seals but let's take a look if the titling pad bearing can actually act as source of instability. After the overhaul in which the bearings were replaced, the 125MW hydro-generator unit started to develop high level of vibrations in the lower generator bearing, brg. No. 2 (Fig. 38).

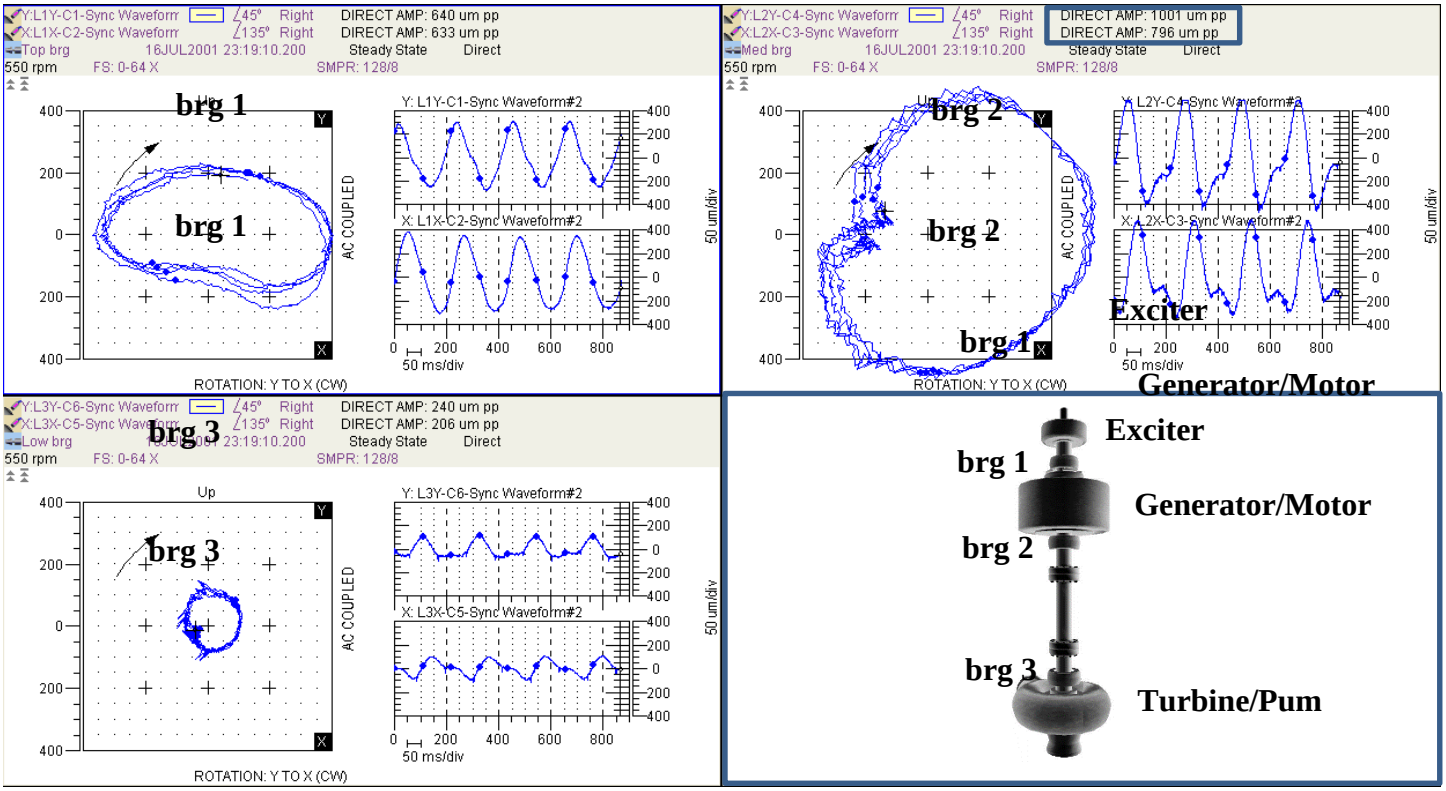

Fig. 38. Instable orbits (½X vibration) in bearings of hydraulic turbine/pump 125 MW train.

All three radial bearings are tilting pad ones, bearing 1 is a combined radial and axial bearing. The machine operates for both directions of rotation (in generation and in pump service), so the pads are supported in the middle. As seen in plots the vibrations are dominated by exactly ½X component (the position of the keyphasor dots are locked, they do not change position with successive cycles) , forward in precession and the levels in bearing 2 are up to 1mm pp (40 mils pp) and they are exceeding the bearing clearance. This is not uncommon for this class of machine; the reason is the construction of the guide bearing (i.e. radial bearing) that is not designed to carry high loads and it has relatively flexible enclosure in which pads are assembled. Looking for the means to stabilize the unit (which was stable in the past) the diagnostic engineer found that some years earlier the bearing clearances were increased (from 0.22 mm to 0.27 mm radial clearance) for bearing 2. That was done in attempt to reduce the casing absolute vibration that was the result of coupling geometry error. The machine was stable after this change, until the last overhaul, but diagnostician followed standard recommendation (load bearing in nominal way) and requested reduction of the clearances to nominal values. The recommendations were completed, and this stabilized the machine operation, but that was not an answer as to what could be the root cause of the problem, so the investigation continued. Another reason considered was that restoring the nominal clearances caused an increase in the bearing metal temperatures which became close to alarm limit. Literature (Frene et al. [15]) shows that in the case of insufficient mechanical preload in tilting pad bearings, unstable vibration can develop, and that the frequency of this vibration is asymptotic to 0.5X (note however that the literature data were for 4 pad bearing, and in this case the bearing is with 12 pads).

Mechanical preload is the geometry parameter defined in Fig. 39

(1) mechanical preload:

$$m = \frac{C_p - C_a}{C_p} = 1 - \frac{C_a}{C_p}$$

where:

m – mechanical preload

C_p – clearance for which the pad is manufactured (i.e. radius of the pad, R_{pad} is shaft journal radius R_s plus C_p)

C_a – clearance for which the pad is assembled

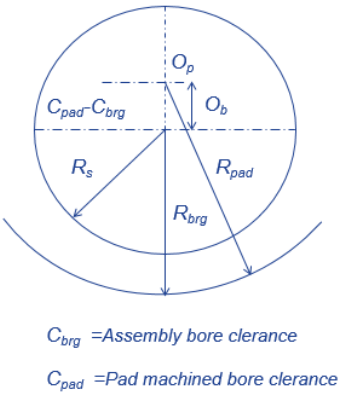

Fig. 39. A depiction of mechanical preload.

Typical values for mechanical preload in horizontal machinery are 0.2 to 0.6 but for vertical machines they can be higher than 0.8. For the unit in question it occurred that the preload of the new pads was marginally above 0 and for increased assembly clearance it became close to zero or even negative. New pads were manufactured with a preload 0.8 and in spite of some earlier concerns that it may cause an increase of bearing metal temperature they proved not only stable but also to have lower temperatures, due to better flow condition. Note that to develop wedge the pad must take proper position to create converging space. With too small mechanical preload there was no stable position of the pad to create converging space for oil flow, so the pad or actually all pads were oscillating.

The lesson learned was to not exclude the tilting pad bearing as the source of unstable behavior and this lesson calls for verification of actual bearing geometry. It was confirmed in many cases for bearings with asymmetrically supported pads when the bearing is installed opposite direction or the shaft starts to rotate in direction opposite to one it was designed for. As a side note – the initial solution provided by the diagnostician was "load the bearing correctly", so we can see that this simple rule also worked here, although not exactly in the way it was thought for fixed geometry bearing.

In the examples we covered so far, the subsynchronous vibration excited by fluid induced instability was always forward in precession i.e. trajectory of developed shaft motion was in direction of shaft rotation. This seemed to be the only possibility because the fluid is put in motion by the rotating shaft, so the wave of the fluid will develop in the forward direction. The data collected for the 60 MW, 3000 rpm steam turbine, a newly built unit under commissioning, indicated an apparent violation of this rule. The turbine was unstable for steam flows higher than 70% of the nominal load, the vibration increase was caused by subsynchronous component with the frequency matching rotor first lateral mode at 1200 cpm i.e. ~ 0.4X, when on nominal speed. But the orbit shapes were far from being circular or elliptical and the reason for that was the subsynchronous frequency being reverse, in both bearings (Fig. 40).

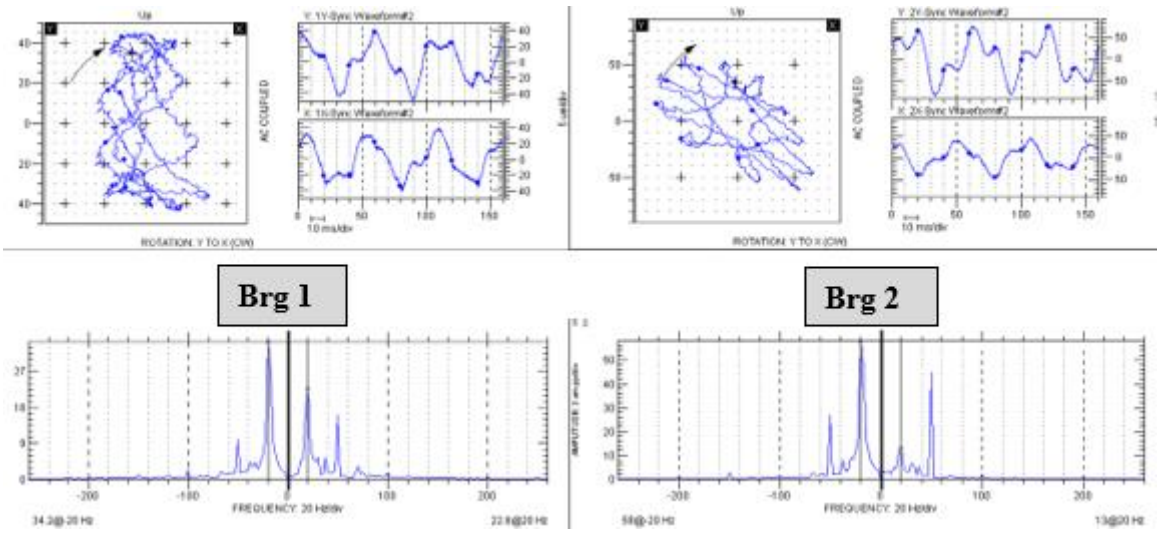

Fig. 40. Unstable orbits and corresponding spectra in bearings 1 and 2 of 40MW steam turbine.

The turbine was equipped with elliptical bearings and the OEM was trying to make it stable by increasing the ellipticity factor from standard 2.5 to 5 (hyper elliptical bearing). However, considering what we learned so far, it should be clear that the source of instability cannot be in the bearing – wave of oil in the bearing would cause forward vibration. The location concluded by the diagnostic engineer was in the long labyrinth seal of the HP turbine. Phase analysis for forward filtered vibration was performed and showed no lag between the two bearings which was expected for any source that is not in the bearing itself. Pointing to the seal as the location can also explain the mechanism of the observed reverse precession. Consider the rotor with some overhung mass and supported in anisotropic bearings, as the one in Fig. 41. Note that this is not a model of the actual rotor because the model was not provided by OEM but it is a simple model of a rotor kit that was used for demonstration of mixed mode.

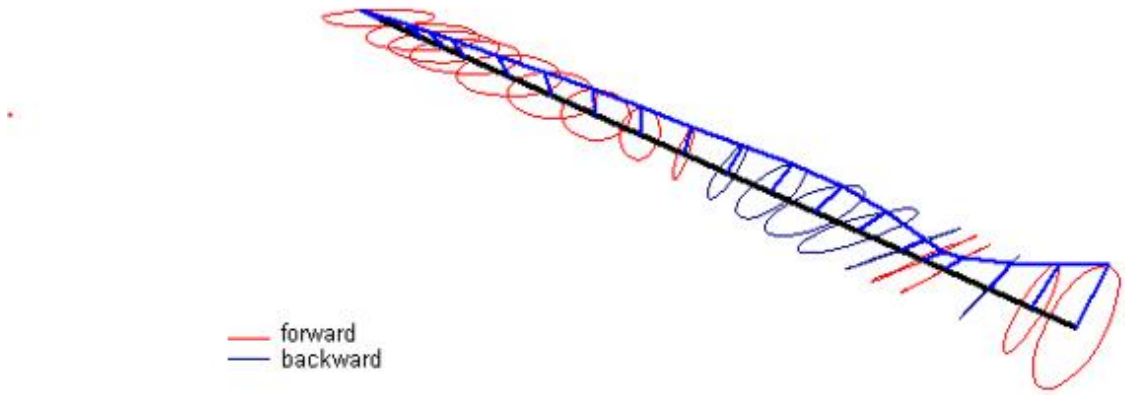

Fig. 41. Mixed mode for rotor kit with an overhung mass, a mass between bearings and anisotropic bearing stiffness.

Mixed resonance mode, the result of rotor and mass and stiffness and the support stiffness is not uncommon for contemporary rotors and it means that when this resonance mode is excited by unbalance (forward excitation), part of the rotor vibrates backward i.e. in reverse direction. Now consider that you are exciting this mode by forward whirling in the seal which is at the location of this backward area. So, on the operating speed, in the unstable condition, we are observing forward 1X vibration as caused by unbalance and the reverse subsynchronous resonance mode (reverse at the bearing location) excited by forward excitation in the seal. Stability calculation performed by OEM confirmed that the design was unstable but because of costs the OEM decided to implement hyper elliptical bearings rather than modify the labyrinth seals. That stabilized machine and unit was accepted for operation. However, the highly loaded bearings were causing so many operational problems that after warranty period the End User decided to commission third party to restore original bearings and to replace the end seal on HP side with the honeycomb one. This finally solved the problems with unstable operation.
This case showed the importance of rotordynamic model both to diagnose the machine problem and to test the solutions. Another lesson learned was that success of stabilizing the machine by use of overloaded bearings may be superficial. Considering that model calculations were clearly showing advantage of more stable seal (which it was rejected as more expensive until the increasing operational costs corrected economic calculation), this is actually the same lesson.

When talking about practical approach to fluid induced instabilities it is important to mention about typical "impostors" i.e. phenomena that in industry cases are sometimes improperly recognized as fluid induced instabilities with all the negative consequences of such a mistake i.e. costs of improper actions. The re-excitation of rotor resonance by subsynchronous component was in some cases wrongly attributed to be bearing instability and "more stable bearing" was requested, although with proper diagnostic methodology the problem was correctly diagnosed either as light rub effect or looseness in the bearing support. Note that incorrect conclusions are typically issued in situations when the analysis is based on incomplete data, for instance data limited to vibration spectrum only. With the use of the full set of fluid instability symptoms, as defined above, it is relatively easy to differentiate between these two groups of self-excited vibrations: fluid induced and the forced subsynchronous ones. Bently [16] refers to this as Mathieu normal to tight (light rub case) or Mathieu normal to loose condition (looseness in the bearing support, poorly lubricated oversized bearing cases) to recognize that problem can be tracked back to description of problems in nonlinear mechanics pioneered by Mathieu E. and others. The key is nonlinear stiffness of the support, that causes excitation of fractional components (natural fraction, either subharmonic ½X, $^1/_3$X, ¼X or more rarely simple integer ratio $^2/_3$X, ¾X and so on) for the speed ranges close to reciprocal of this fraction. I.e. if due to light rub the dynamic stiffness increases for part of vibration cycle (Fig. 42a) the ½X and its harmonics can appear when rotor speed is above 2 times resonance speed and $^1/_3$ X with possible harmonics, when it is more than 3 times the resonance speed. For oversized bearing with unbalance or for the looseness in the support (Fig. 42b) the same fractional components will be generated for speeds below nX resonance speed. Note that there can be small problem with naming – this is self-excited fractional component due to forced action of 1X, so referring to this

vibration as forced or self-excited are both correct.

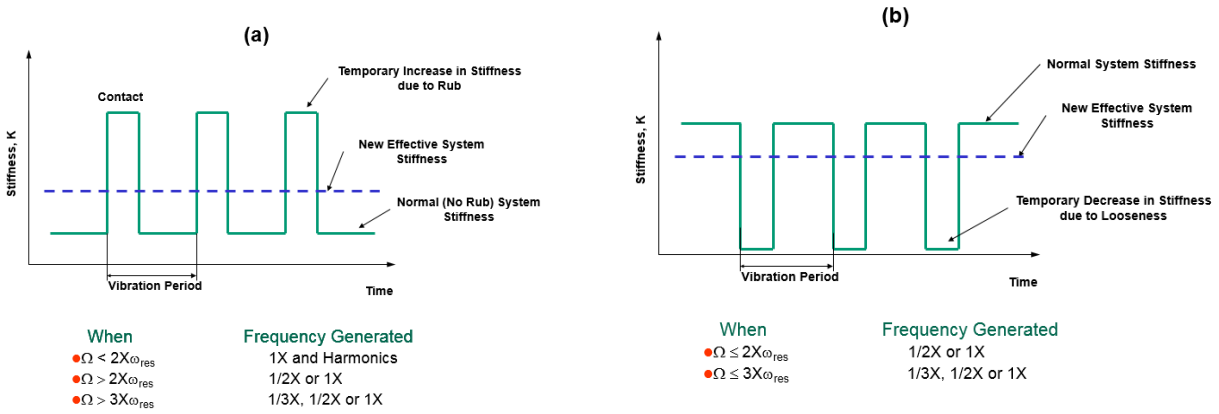

Fig. 42. Periodic change of stiffness in the Mathieu normal-tight (a) and normal-loose (b) condition with typically generated vibration components.

During the diagnostic training, the partial rub condition is demonstrated using rotor kit with a rub screw (Fig. 43) and the students are learning to recognize the forced subsynchronous action vs. the fluid induced instability situation.

The following differences are underlined in case of re-excitation of the resonance by fractional component:

- The frequency is natural fraction of the rotating speed, so in synchronous waveforms the keyphasor events will be at the same moment of the cycle and the keyphasor dots in the orbits will maintain stable position in particular revolutions. Note that this is not always possible to see the frequency difference in spectra due their limited resolution. Care should be taken to not make the conclusion from single sample as the transient condition can make keyphasor dot pattern "smeared" for some time periods.

- There is relationship between the range of machine speed the subsynchronous vibration appears and the rotor resonance speed because the excited frequency is rotor resonance frequency, although modified to be higher than normal by rub or to be lower because of reduction in support stiffness. However, it should be recognized that the stiffness can be modified for some other reasons. For example, it is normal that position in the bearing is different when the machine passes the resonance during transient and on the n times higher speed when $^1/_n$ X subsynchronous action occurs. As a result, it is not always easy to distinguish between normal tight and normal loose condition. One practical observation is that whether rub can happen both for high and low values of 1X component, in the case of looseness in horizontal machinery we need reasonably high 1X (i.e. enough of unbalance force) to temporarily lift the rotor in the bearing. Therefore, presence of fractional component without significant 1X should be attributed to rub action, when with presence of considerable 1X it can be both for rub or looseness. Experience shows however that subsynchronous component can be forward (or reverse) but generally is not circular or slightly elliptical like in most of the cases of fluid induced instabilities. This can be seen in orbits and full spectra but is easy to miss if the plain spectrum is used.

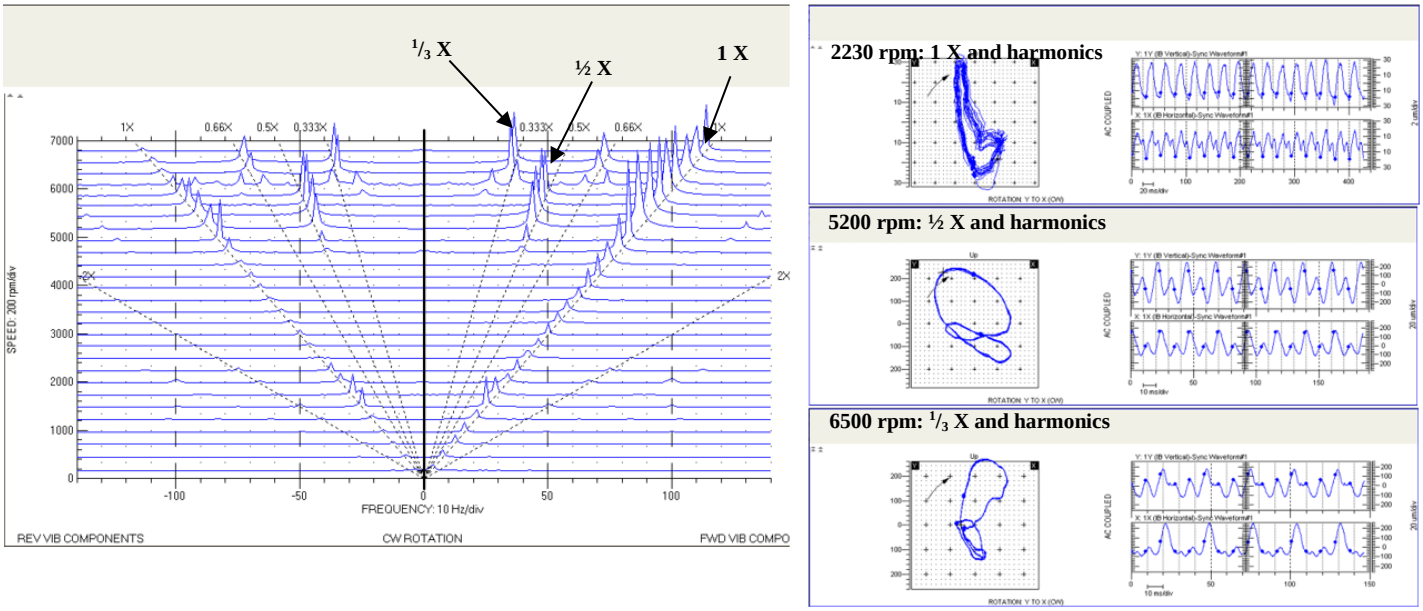

Fig. 43. Full spectrum cascade from rub test on rotor kit, orbit-timebase plots with 1X and harmonics, ½X and harmonics and 1/3X and harmonics, depending on actual speed vs. resonance speed.

The value of rotor kit demonstration lies in the fact that students can see subsynchronous vibration patterns generated on the machine in which there is no fluid bearing and no other gas or fluid action can be claimed.

Let's take a look at two examples of forced subsynchronous action in full size machines.

The 30 MW, 3000 rpm steam turbine generator train shown high (10 mils pp) vibration during the startup following overhaul. During this overhaul front generator bearing was replaced by new one but of the same type as the original one.

Generator rotor resonance, as observed during transients was at 1340 rpm. During machine startup the subsynchronous component, forward in precession and with frequency exactly ½ X is generated when rotor speed is ~ 2700 rpm or higher. The cascade plot in fig. 17 shows when subsynchronous action is present, but orbit-timebase plots should be checked to see the locked dot pattern (exactly 2 keyphasor dots visible for 8 shaft revolutions) and flat part of orbits showing angular location of the rub. Note that the orbits for lower speeds, including the speed 2680 rpm (exactly 2 times resonance speed as observed in transient) are showing the same location of limitation in shaft trajectory, suggesting that rub is already present at lower speeds, but the subsynchronous component appears only for speeds exceeding 2 times resonance speed (Fig. 43). The orbit pattern illustrates mechanism of the subsynchronous action – for lower speeds the rotor is in contact with the stationary part once per revolution but when the resonance mode is re-excited the energy delivered during the contact pushes the rotor away (the rotor is re-bounced away) from the contact spot and for one revolution is not contacting the stationary part. Bently [1] describes this effect as similar to pushing the child on a swing. When the push (the transfer of energy) is applied, the child moves away, acting as a pendulum in free vibration. The key is correct timing of delivering impulses and the amplitude of "swing" will greatly increase.

The shaft centerline plot suggests that there is still enough clearance in the bearing, but on the other hand the subsynchronous component orbits are not "flat" (i.e. with forward and reverse part on the full spectrum of similar amplitude, representing high ellipticity of filtered orbit - compare proportions of forward and reverse component of fractional components in Fig. 43 and in Fig. 46). Also, the direct orbits do not have external loops characteristic for dry rubs (Fig. 43). Friction force is tangential component acting against rotation, so if this component is strong enough it causes part of the trajectory to be reverse, but this is not visible in this case. Based on the above characteristics the diagnostic engineer concluded heavy rub condition, but most likely lubricated one, and recommended inspection of upper half of the bearing. Inspection confirmed error in manufacturing – one of the surfaces close to the bearing seal was machined eccentric, causing reduction of the clearance in upper-left quadrant of the bearing. Machine was started with old bearing and the new one was sent back to workshop for the geometry correction.

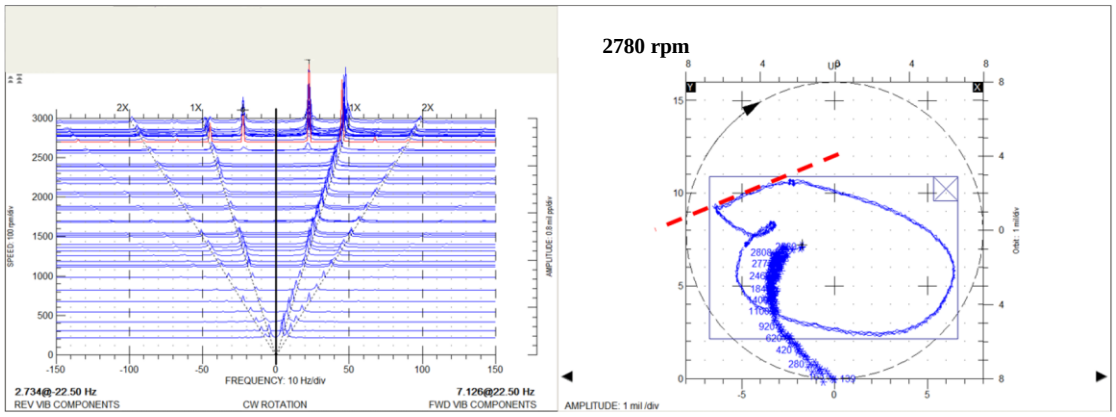

Fig. 44. Full spectrum cascade plot and shaft centerline plot with orbit overlay for lubricated rub condition in 30MW generator bearing. Dashed line shows expected position of the rub contact in the bearing.

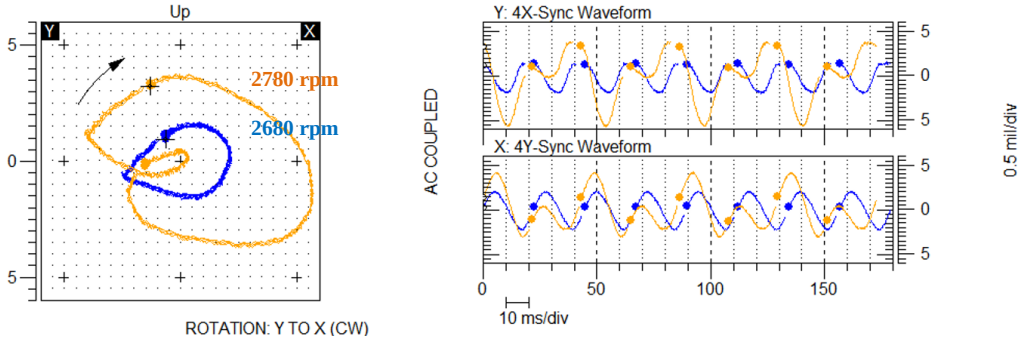

Fig. 45. Sample orbits for rub condition, when rotating speed is exactly 2 times resonance speed (blue, one Keyphasor dot) and for speed higher than 2 times resonance speed (orange, two Keyphasor dots).

Equipped with the gathered knowledge we can take a look at the data collected for a 300MW, 3600 rpm generator. The front generator bearing vibration increased when generator was loaded for more than 50% of nominal load. Four stationary keyphasor dots in orbit (Fig 46) are suggesting that at 3600 rpm we are operating close to 4 times resonance speed, but exact location of resonance was initially not available because during the startup machine passes resonance region very quickly, as a part of normal startup sequence.

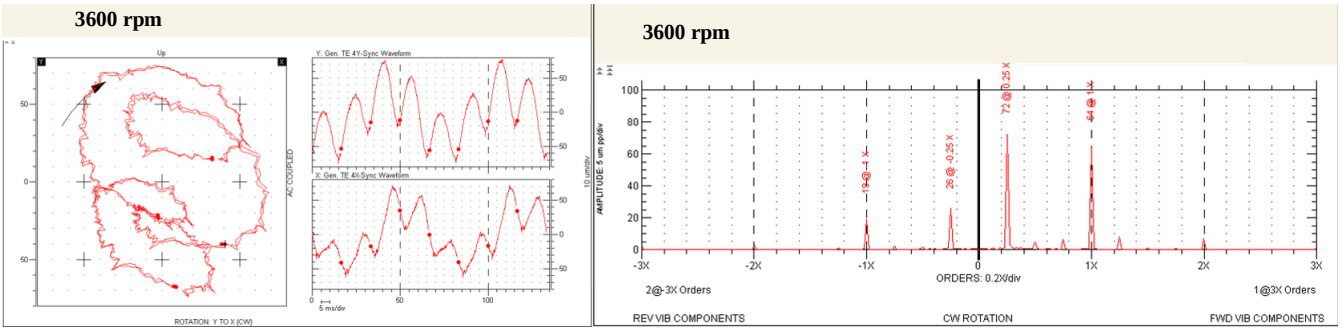

Fig. 46. Orbit-timebase and full spectrum sample for ¼ X subsynchronous action in generator front bearing.

The 1X component (on level ~ 3.3 mils pp) is considered significant enough comparing to subsynchronous ¼ X (at ~ 3.9 mils pp), so we cannot exclude neither normal-tight nor normal-loose action. Evaluating shaft centerline plot with orbit overlay (Fig. 47) the diagnostician concluded that the direction of the motion during free vibration part of the cycle is in the direction of the lowest clearance which is rather unexpected result if rub is assumed. However, it is normal for looseness in the support assumption, as the unbalance force can unload the bearing when pointing up during half of the shaft rotation and load it more for the other half of it, so the trajectory of motion for the reduced stiffness (free vibration) part of the cycle can be above the normal stiffness part of the cycle.

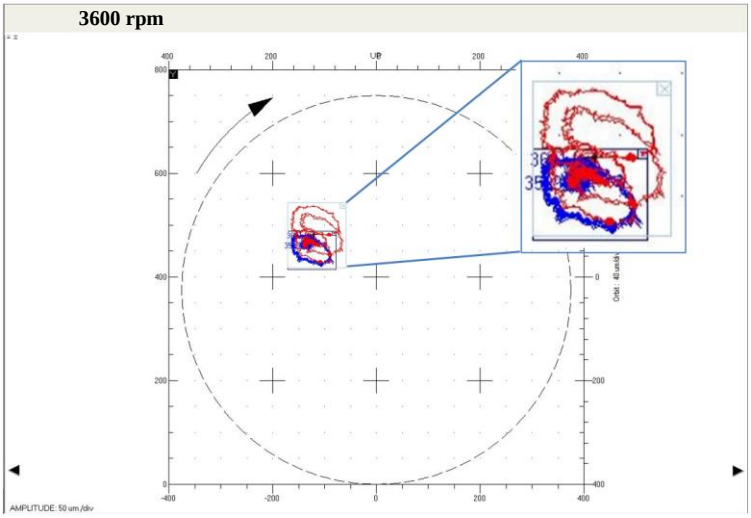

Fig. 47. Shaft centerline plot with orbits overlaid. The stable orbit (blue) and the excited forced subsynchronous ¼X (red). Observe the part of the cycle that is common for both orbits and direction of the free vibration part of the cycle.

The recommendation was to stop machine for alignment check as the bearing load was considered low (based on comparison with shaft centerlines in the adjacent bearings). Additional recommendation was to check the bolt torque in the bearing support and cover, which was done before shutdown. Fig. 48 shows ceasing of the subsynchronous excitation at the moment one of the bolts was tightened. The shutdown confirmed resonance speed to be 930 rpm (Fig. 49). So, at operating speed the unit was working slightly below 4 times resonance speed, as expected for normal-loose condition.

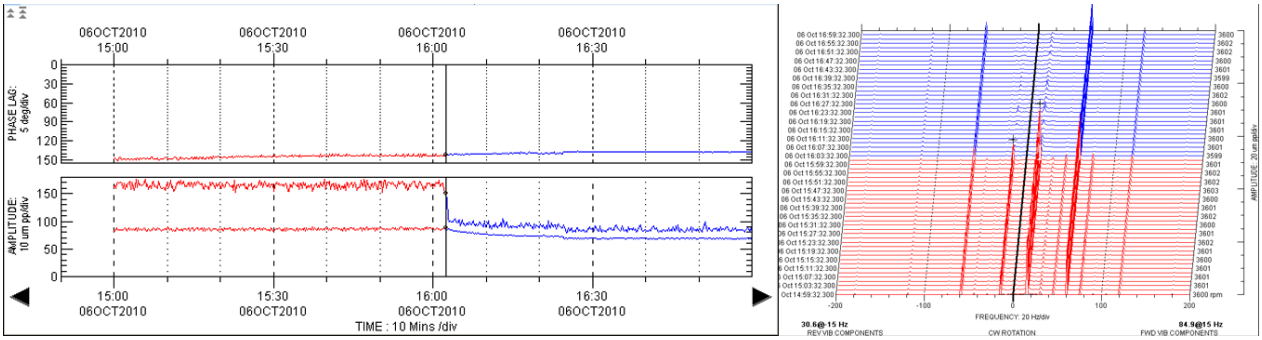

Fig. 48. Vibration trend and full spectrum waterfall showing the ceasing of subsynchronous action when the bearing support bolt was tightened.

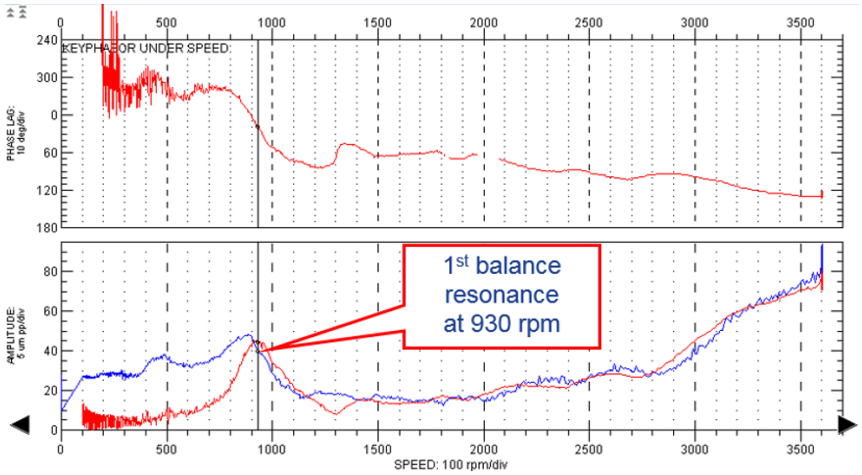

Fig. 49. Bode plot for shutdown of the unit showing the resonance speed at 930 rpm so the subsynchronous action at 3600 rpm was at speed slightly below 4 times resonance speed.

From the above examples it can be seen that distinguishing between fluid induced instabilities and their "impostors" i.e. the parametric vibration phenomena due to nonlinearity of stiffness, is not very complex task, providing that analysis is including more than simple check of vibration content.

In summary of the self-excited vibration section authors would like to point to importance of proper identification of source of unstable behavior as too often bearing whirl/whip is claimed based solely on presence of subsynchronous component in the vibration. Once the source if instability is identified the decision to bring the system to original condition, or to modify it, is made. In this latter case the computer models proven to be safe and economic way of making decision about design changes rather than forcing the use of "more stable bearing design" in each and every case.

SUMMARY

Machinery malfunctions represented by either forced vibration (shaft crack) or self-excited vibration (fluid film induced instabilities and forced subsynchronous excitations) are presented to demonstrate that a proper diagnostics methodology allows solving machinery dynamic problems even if *the* machine apparently "fails" to follow rules stated in (some) diagnostics manuals.

The controversial title of the tutorial was based on the typical claim of the adepts of diagnostic trainings that actual field data do not look the same way as it was presented in a manual or as it was demonstrated in a test rotor kit during the diagnostics training.
However, being active industry diagnosticians and instructors, the authors learned that although machines probably do not read some of the rotordynamic literature (we apologize for the joke), when closely observed, these machines openly avoid to break physical laws.
We should rather teach students to use data and dynamic models to explain machine behavior. The conclusion is nothing new for the audience of industry conferences, so the message is re-stated and enforced by some examples of machinery behavior.

References

[1] Bently, D., E., Hatch C., T., Grissom, B.; Fundamentals of Rotating Machinery Diagnostics, Bently Pressurized Bearings Press 2002.

[2] Lapini G. L., Zippo M., Bachshmid N., Collina A., Vallini A., Experimental Tests and Model Based Calculations for the Diagnosis of a Crack in 320 MW Generator, Diagnostics of Rotating Machines in Power Plants, Proc. CISM/IFToMM Symp. Oct. 27-29 1993 Udine Italy, Springer-Verlag 1994.

[3] Eisenmann Sr., R. and Eisenmann Jr. R. (1998): Machinery Malfunction Diagnosis And Correction. Upper Saddle River, NJ: Prentice Hall PTR.

[4] Muszynska, A. (2005): Rotordynamics. CRC Taylor & Francis Group, ISBN 0-8247-2399-6, Boca Raton, London, New York, Singapore, pp. 1-1120.

[5] Dimarogonas, A.D. (1996): Vibration of cracked structures: A state of the art review, Engineering Fracture Mechanics, Volume 55, Issue 5, pp. 831-857.

[6] Gasch, R. (1993): A survey of the dynamic behavior of a simple rotating shaft with a transverse crack, Journal of Sound and Vibration 160, (2), pp. 313-332.

[7] Bachschmid, N., Pennacchi, P., Tanzi, E., Vania, A. (2000): Identification of transverse crack position and depth in rotor systems, Meccanica 35 (6), pp. 563–582.

[8] Bachschmid, N., Pennacchi, P., Tanzi, E. (2010): Cracked Rotors, Springer, Berlin.

[9] Popálený, P. (2013): Rotor Crack Diagnostics Using Vibration Measurements and Model Based Approach, Dissertation Thesis, Bratislava, Slovakia.

[10] Allianz Handbook of Loss Prevention, VDI Verlag 1987.

[11] Allianz Berichte für Betriebstechnik und Schadenverhütung Nr 24: Schwingungsüberwachung von Turbosatzen – ein Weg zur Erkennung von Wellenrissen, full discussion report (in German), May 1986.

[12] Sohre, J., S., Turbomachinery Problems and Their Correction, 1980.

[13] Bently, D.E, Goldman, P., and Yu, J. J., The Advantages of Dynamic Stiffness Parameters Over Classical Bearing Coefficients, *Orbit* 3 (2001): 23-28

[14] Bently, D., E., Bosmans, R., F., A method to locate the source of a rotor fluid-induced instability along the rotor, ISROMAC-3, 1990.

[15] Frene, J., Nicolas, D., Degueurce, B., Berthe, D., Godet, M., Hydrodynamic Lubrication – Bearings and Thrust Bearings, ELSEVIER 1997.

[16] Bently, D. E., Forced Subrotative Speed Dynamic Action of Rotating Machinery, ASME Conference Paper 74-Pet-16.